

Latent Performance Profiling of Large Language Models

Tanmoy Chakraborty^{*1,2}, Ayan Sengupta¹, Suparna Bhattacharya³, Partha Pratim Chakrabarti⁴, Amlan Chakrabarti⁵, Supratik Chakraborty⁶, Partha Pratim Das⁷, Lipika Dey⁷, Richa Singh⁸, and Mayank Vatsa⁸

¹Department of Electrical Engineering, Indian Institute of Technology Delhi, New Delhi India

²Yardi School of Artificial Intelligence, Indian Institute of Technology Delhi, New Delhi India

³Hewlett Packard Enterprise, India

⁴Department of Computer Science & Engineering, Indian Institute of Technology Kharagpur, India

⁵A.K.Choudhury School of Information Technology, University of Calcutta, India

⁶Department of Computer Science & Engineering, Indian Institute of Technology Bombay, India

⁷Department of Computer Science, Ashoka University, India

⁸Department of Computer Science & Engineering, Indian Institute of Technology Jodhpur, India

ABSTRACT

Large language models (LLMs) frequently achieve impressive scores on standardized benchmarks, yet accuracy alone offers a limited view of their capabilities. Evaluating open-source LLMs through leaderboards faces persistent issues like data contamination, narrow task scope, and weak alignment with real-world reliability. Benchmark-based evaluations such as MMLU PRO, BBH, or IFEval primarily capture *what* a model outputs on fixed test sets, not *how* it processes information, calibrates uncertainty, or structures internal knowledge. In this article, we advocate for a shift from benchmark-centric evaluation toward a complementary, *state-centered intrinsic assessment* of LLMs. To this end, we introduce **Latent Performance Profiling (LPP)** – a framework that derives task-agnostic diagnostics from hidden activations and output distributions. LPP defines a set of scalar metrics on a model’s latent representations and dynamics, revealing scale-independent traits that enable interpretable comparisons and uncover hidden vulnerabilities. Unlike static accuracy scores, LPP provides stable, architecture-sensitive signatures across models of similar size. With extensive empirical analyses across eight LLMs, spanning a size range of 0.5B-14B, we demonstrate that models with similar benchmark scores can exhibit contrasting latent profiles, such as differences in entropy or adaptability. Guided by these insights, we design synthetic probes for uncertainty and symbolic reasoning that align with intrinsic metrics while decoupling from leaderboard bias. We recommend that reporting LPP alongside benchmarks provides a deeper, interpretable understanding of model behavior, enabling more reliable model selection, safety assessment, and evaluation beyond surface-level accuracy.

As large language models (LLMs) continue to dominate public leaderboards (Chang et al., 2024; Liang et al., 2023), concerns are growing that such leaderboard-driven evaluations conflate genuine reasoning ability with brittle, surface-level pattern recognition (Farquhar et al., 2024). Recent open-source models, such as LLaMA, Qwen, Mixtral, and Mistral, approach or match the performance of proprietary systems across various domains, including knowledge tasks, reasoning, and code generation, and are increasingly deployed in critical real-world applications (Boiko et al., 2023; Milano et al., 2023; Miret and Krishnan, 2025; Xin et al., 2025). However, key questions remain about how these models internally process information and whether existing benchmark accuracy meaningfully reflects underlying capability or reliability. Most leaderboards, such as those built on MMLU (Hendrycks et al., 2021), GSM8K (Cobbe et al., 2021), and HumanEval (Chen, 2021), report performance on fixed, task-specific test sets. To expand coverage, newer evaluations such as MMLU-Pro (Wang et al., 2024), IFEval (Zhou et al., 2023), and BIG-bench (Srivastava et al., 2023) target multi-step reasoning, instruction following, and social cognition. While these advances improve task coverage, they remain extrinsic and evaluate only final predictions, not the model’s internal decision-making process.

This output-only focus limits interpretability and reliability. Leaderboard gains are often inflated by data contamination (Sainz et al., 2023), prompt engineering, or overfitting to benchmark-specific patterns (Banerjee et al., 2024). Furthermore, Goodhart’s Law suggests that once benchmarks become optimization targets, they lose diagnostic utility (Fodor, 2025). Despite high scores, models continue to hallucinate, fail under distribution

^{*}Corresponding author: tanchak@iitd.ac.in. First two authors contributed equally. The remaining authors are listed in chronological order by surname.

shift, and exhibit brittle reasoning. Core competencies such as uncertainty calibration, robust compositionality, or structured reasoning remain largely unmeasured.

These limitations are further highlighted by inconsistencies among models of comparable scale and complexity. A 70B-parameter model may excel at code generation, whereas another of comparable size may perform better in dialogue or reasoning. Public leaderboards collapse such nuanced differences into a single composite score, obscuring meaningful variation. Although scaling trends suggest that performance generally improves with model size (Jha and Reagen, 2025; Wei et al., 2024), this relationship can be misleading. As Fodor (2025) argued, progress on narrow benchmarks does not necessarily imply broader generalization. Empirical analyses reveal brittle internal representations, where trivial perturbations in input can derail outputs (Haller et al., 2025). Moreover, genuinely emergent abilities tend to appear only beyond specific scaling thresholds, below which performance may stagnate or even regress. Consequently, benchmark metrics often provide an incomplete and sometimes distorted view of model capability.

In this article, we argue for moving beyond benchmark-centric evaluation and adopting a complementary, state-centered intrinsic framework for assessing LLMs. We propose **Latent Performance Profiling (LPP)** as a complementary framework for evaluating LLMs. Unlike traditional benchmarks, LPP probes *how* a model processes information by measuring internal dynamics – specifically, predictive uncertainty, representational compression, and activation diversity. We introduce three task-agnostic metrics: minimum next-token entropy (calibration), effective rank of hidden-state covariances (dimensionality), and participation ratio (variance distribution). These metrics, computed on unlabeled prompts, form compact latent profiles that are robust across context lengths, model scales, and datasets. Crucially, LPP reveals performance-relevant traits invisible to benchmark accuracy.

Our empirical analyses span open-source LLMs with parameters ranging from 0.5B to 14B, encompassing the LLaMA, Qwen, and Mistral families. We find that models with similar benchmark accuracy (e.g., on IFEval or BBH) diverge widely in LPP space, exhibiting distinct uncertainty floors and activation geometries. Our results show how two models – Mistral-7B and Qwen-7B, achieve comparable accuracy but differ in entropy and representational spread, indicating fundamentally different reasoning strategies. Layerwise analysis further reveals an emergent hourglass structure across models: shallow and deep layers exhibit high entropy and dimensionality, while middle layers form compressed bottlenecks.

To demonstrate the practical value of LPP, we introduce two synthetic diagnostic tasks – Ambiguous Reasoning (AR) and Symbolic Pattern Completion (SPC), designed to stress-test entropy calibration and representational compression. Performance on these tasks correlates strongly with corresponding LPP metrics and separates models more clearly than traditional benchmarks. Figure 1 illustrates that LPP unveils substantial variation among models with superficially similar benchmark scores. For example, one model may display low entropy and high plasticity, indicating confident, adaptable reasoning (Farquhar et al., 2024), while another may exhibit high entropy and redundant internal states, suggesting fragility despite comparable accuracy. In this work, we formalize such latent behaviors through a set of interpretable LPP metrics and provide a detailed empirical analysis of how these internal patterns vary across model families, sizes, and inputs. While our proposed metrics – entropy, participation ratio, and effective rank, are not exhaustive, they offer a principled starting point for state-based evaluation. We view LPP as a “litmus test” that probes essential internal properties of LPP, offering complementary insight to traditional benchmarks and motivating the development of more comprehensive latent evaluation frameworks in the future.

Results

Benchmark performance inconsistencies

LLMs are primarily evaluated on public leaderboards such as MMLU (Hendrycks et al., 2021), GSM8K (Cobbe et al., 2021), and HumanEval (Li et al., 2025), which track general knowledge, mathematical reasoning, and coding ability, respectively. While these benchmarks indicate steady progress, they often conceal structural limitations, including data contamination (Sainz et al., 2023) and overfitting driven by Goodhart’s Law (Banerjee et al., 2024). Newer suites broaden task coverage but still offer limited insight into a model’s reasoning processes or robustness. Moreover, models frequently rank differently across leaderboards, leaving practitioners uncertain which model to deploy for a given application.

To quantify these inconsistencies, we benchmark eight open-source models – LLaMA-3B, LLaMA-8B, Qwen-0.5B, Qwen-1.5B, Qwen-3B, Qwen-7B, Qwen-14B, and Mistral-7B, on three representative suites: MMLU-PRO, IFEval, and Big-Bench Hard (BBH), covering knowledge, instruction-following, and multi-step reasoning. As expected, larger models generally achieve higher accuracy, consistent with established scaling laws (Hernandez et al., 2021; Kaplan et al., 2020). However, size alone is an unreliable predictor of leaderboard performance. For instance, Qwen-3B outperforms Mistral-7B on the IFEval test (55% vs. 45% accuracy; Figure 2A) despite having fewer parameters.

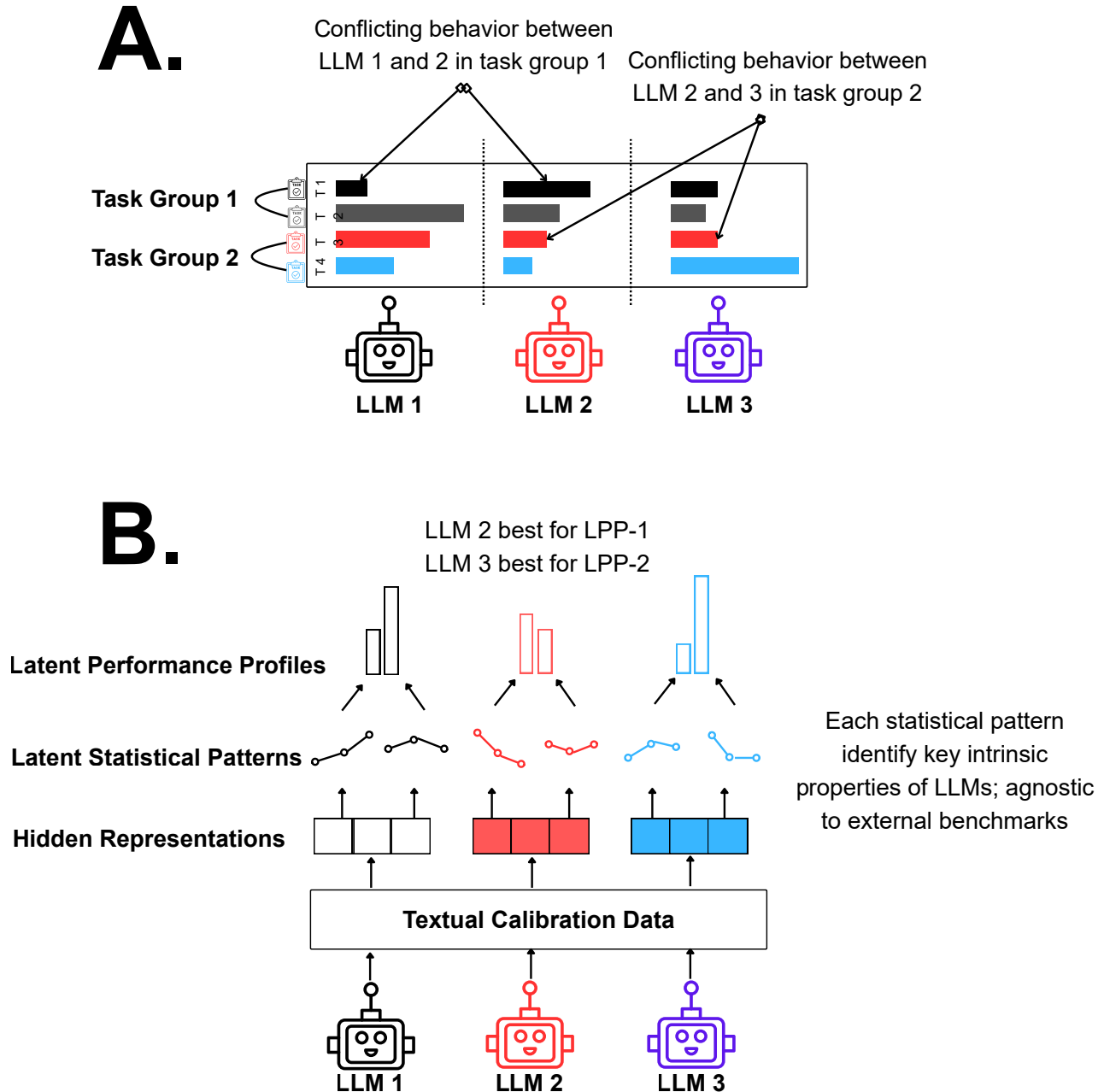


Figure 1. Our proposed framework – Latent Performance Profiling (LPP), aims to uncover differences in LLM behavior that extrinsic benchmarks may miss. While traditional evaluations might suggest similar capabilities across models, LPP probes their *internal activations and representations* to reveal deeper distinctions. (A) We highlight instances where three LLMs are evaluated on four downstream tasks, across two task groups. LLM 1 and 2 demonstrate conflicting behavior in task group 1, wherein one model achieves higher performance in one task, while another excels in the other. These behaviors (empirically highlighted in Figure 3) are *unreliable* for a practitioner selecting a model for a similar new task. (B) LPP-driven benchmarks, grounded in intrinsic statistical patterns, offer more reliable signals. For instance, a model with lowest entropy may be better suited for tasks requiring minimized hallucination risk.

Likewise, Mistral-7B surpasses Qwen-1.5B on IFEval and BBH (55% vs. 45%, and 22.9% vs. 20%, respectively), yet it slightly trails on MMLU-PRO (19% vs. 20%). Even models with nearly identical architectures yield inconsistent rankings: LLaMA-8B scores only 0.2 percentage points higher than LLaMA-3B on IFEval, despite being over twice

the size. At higher performance tiers, recent model families cluster tightly in score (for instance, LLaMA-3 and Qwen2.5 are nearly indistinguishable on these benchmarks; Figure 3A), making it difficult to determine which model is truly superior for real-world tasks.

These findings strengthen the limitations of leaderboard-centric evaluation. Benchmarks are indispensable for measuring task success, but they do not reveal how models arrive at answers or why similar accuracy can stem from divergent reasoning pathways. High aggregate scores often hide failure modes such as miscalibration, brittle intermediate representations, or overly high-dimensional activations that are sensitive to context shifts. This motivates the need for complementary diagnostics that move beyond surface metrics to characterize internal model behavior, latent risk, and reliability.

Latent Performance Profiling reveals hidden differences

To address these shortcomings, we introduce LPP as an intrinsic evaluation framework. Rather than focusing on what answer a model outputs, LPP examines how the model’s certainty and representations evolve internally as it processes information. We define a set of task-agnostic metrics (Table 1) computed from the model’s hidden states and next-token probabilities that serve as proxies for core aspects of its internal computation. In this work, we focus on three such metrics: the *uncertainty floor*, defined as the minimum next-token entropy attained across a prompt (capturing calibration of confidence); the *effective rank* (ER), which estimates the active dimensionality of the hidden representations; and the *participation ratio* (PR), which measures how evenly the variance of activations is distributed across dimensions. These metrics, aggregated per model (specifically using the extremal values: minimum entropy, maximum ER, and maximum PR), provide a compact “latent profile” that characterizes the model’s confidence regime and representational breadth under generic inputs. We elaborate on these metrics in the *Materials and Methods* section.

Using LPP, we profile eight open-source models and find striking latent differences even when benchmark-based external performances are similar. For instance, Qwen-7B and Mistral-7B achieve comparable accuracy on the BBH benchmark (Figure 2A), yet they diverge markedly in their internal metrics (Figure 2B). Qwen-7B has a much lower participation ratio and effective rank than Mistral-7B, indicating that Qwen-7B’s activations reside in a more compact, lower-dimensional subspace despite solving the same tasks. Mistral-7B, by contrast, uses a higher-dimensional and more diffuse representation. In other words, these two 7B-parameter models appear equally capable by external score, but LPP reveals that they employ distinct internal strategies to reach those answers. Figure 3 illustrates this phenomenon more broadly: models with similar benchmark scores can exhibit very different latent signatures. Traditional metrics alone cannot distinguish whether performance gains arise from fundamentally improved latent computation or merely from superficial changes, such as scale or fine-tuning.

Examining LPP metrics across varying prefix and context lengths (Figure 4) further reveals that model families cluster based on their intrinsic behavior. All LLaMA variants display similar entropy dynamics as the input context grows, whereas Qwen and Mistral families form separate groups. This suggests that uncertainty management is governed more by architecture (family-specific traits) than by model size. In a two-dimensional entropy-PR plane, each model occupies a distinct region reflecting its calibration-compression trade-off. Qwen-14B and Qwen-3B, for example, combine low entropy with low PR, indicating highly confident predictions from very compact representations. Mistral-7B achieves the lowest overall entropy (strong confidence) but maintains a moderate PR, whereas Qwen-7B attains the lowest PR (most compressed representations) but at the cost of higher entropy. In contrast, smaller models like LLaMA-3B and Qwen-0.5B exhibit both high entropy and high PR, corresponding to diffuse and uncertain latent states. Crucially, none of these differences is apparent from benchmark accuracy alone. For instance, LLaMA-3B and LLaMA-8B reach nearly identical IFEval scores, yet LLaMA-3B is clearly less calibrated (higher entropy floor) and operates in a higher-dimensional latent space than its 8B counterpart. Together, these observations establish LPP as a principled tool for disentangling performance ambiguities and exposing latent characteristics that conventional evaluations overlook.

Intrinsic metrics versus extrinsic performance

We next assess the extent to which traditional benchmark scores reflect the latent properties captured by LPP. For each model, we compute Spearman correlations between its LPP metrics (entropy floor, max-ER, max-PR) and its scores on MMLU-PRO, BBH, and IFEval (Figure 2D). The resulting correlations are weak or statistically insignificant: across three benchmarks and three intrinsic metrics, Spearman ρ values range from roughly -0.75 to -0.32 , with most correlations not statistically significant (p -value > 0.1). In practical terms, a model’s rank on public leaderboards provides little indication of its uncertainty calibration or representational efficiency. For example, a high-performing model on BBH does not necessarily exhibit a low entropy floor or a compact latent space, and vice versa.

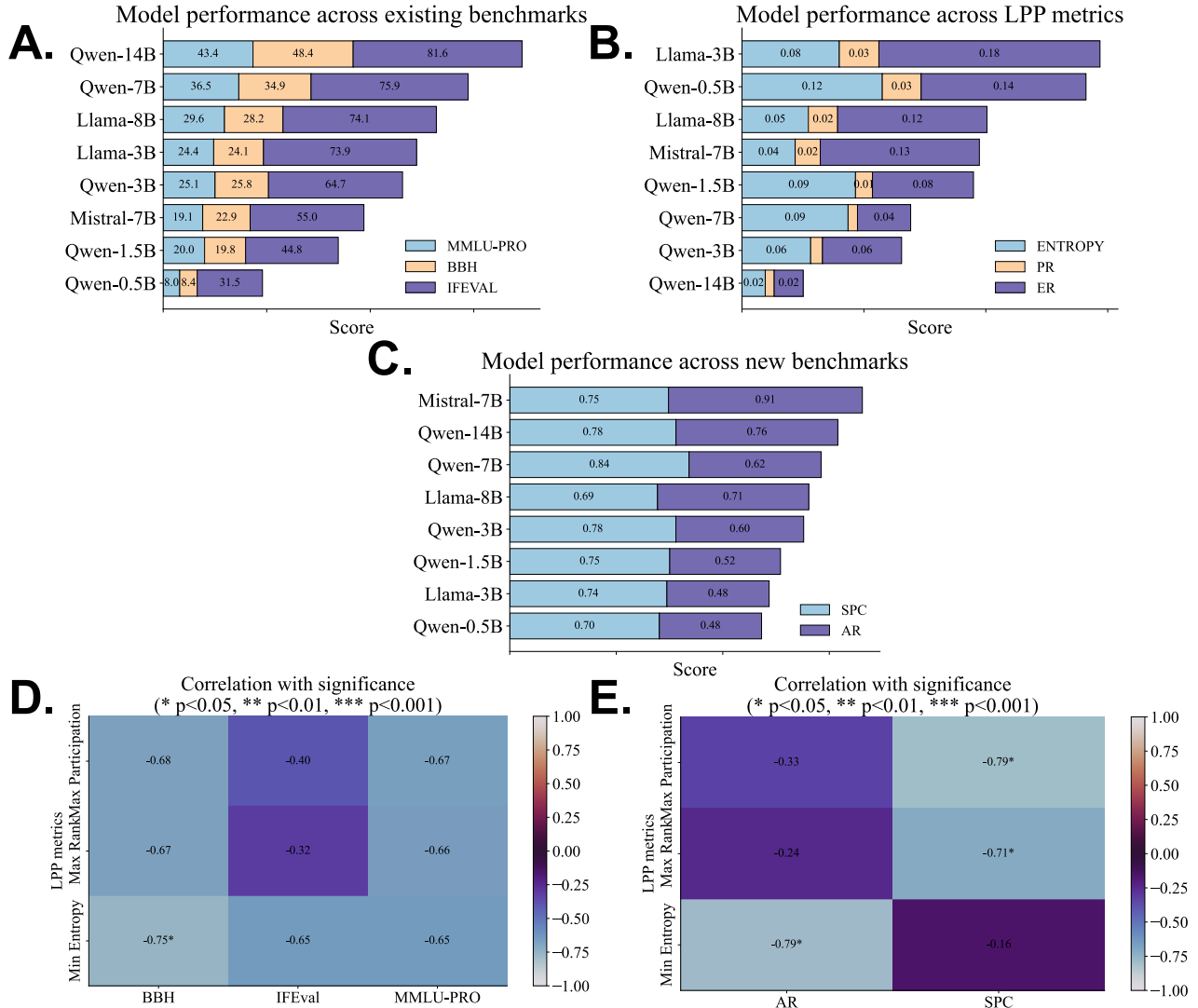


Figure 2. Extrinsic benchmark performance, latent profiling, and correlation with new LPP-driven tasks. This figure summarizes the core empirical findings of our study. **(A)** Comparison of model performance across three widely used extrinsic benchmarks (MMLU-PRO, BBH, and IFEval), revealing size-dependent trends and inconsistency across tasks – larger models do not uniformly outperform smaller ones. **(B)** LPP metrics – Entropy, PR and ER values for different LLMs. **(C)** Performance on two synthetic, LPP-inspired benchmarks – Ambiguous Reasoning (AR) and Symbolic Pattern Completion (SPC), designed to target specific internal capacities (entropy modulation and representation compression, respectively). Unlike standard tasks, these LPP-driven benchmarks show clearer structure across models. **(D)** Pearson correlation between these benchmark scores and intrinsic capacity metrics from Latent Performance Profiling (minimum entropy, maximum intrinsic rank, and maximum participation ratio). Weak or non-significant correlations across most metrics suggest that current benchmarks fail to isolate consistent latent properties and may conflate surface-level accuracy with different underlying dynamics. **(E)** Performance on these synthetic tasks correlates significantly with corresponding latent metrics, especially entropy, validating their interpretability and diagnostic alignment. Together, we show how LPP metrics provide a stable, scale-independent lens to explain heterogeneous model behavior, resolve benchmark ambiguities, and support the principled design of future evaluation tasks.

This disconnect confirms that benchmark scores alone are unreliable proxies for core model behavior. Extrinsic evaluations capture task-specific success, but not attributes like confidence management, internal diversity, or

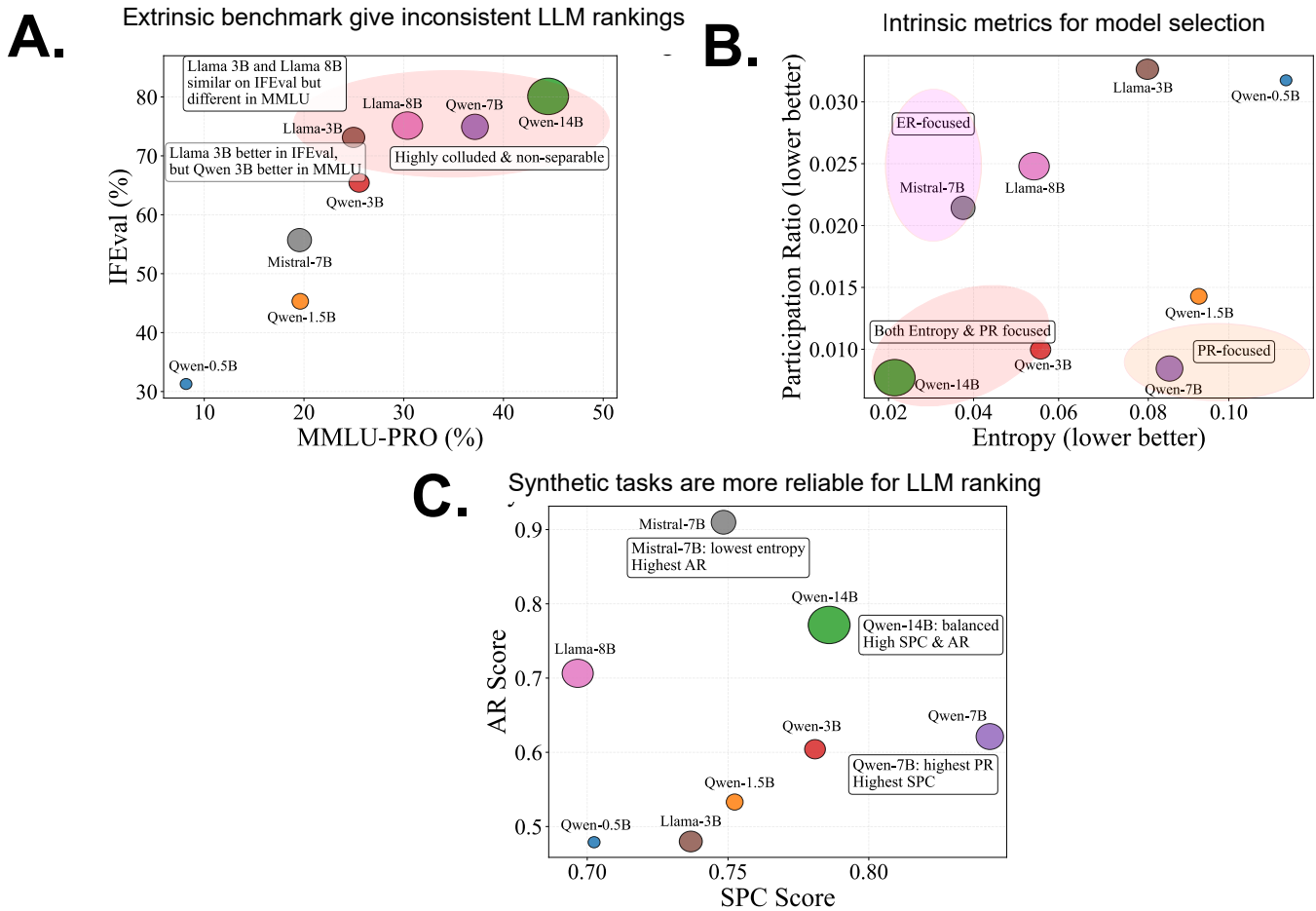


Figure 3. Comparison of (A) extrinsic, (B) intrinsic, and (C) synthetic metrics for LLM ranking. (A) MMLU-PRO vs. IFEval shows inconsistent rankings across models (e.g., Llama-3B vs. Qwen-3B), with a colluded top-right cluster indicating poor separability under extrinsic evaluation. (B) Intrinsic metrics (entropy, participation ratio, effective rank) clearly separate models and offer actionable guidance for selecting models based on stability, activation diversity, or representational richness. (C) Synthetic tasks (SPC, AR) provide a much more stable ordering that aligns closely with intrinsic properties.

robustness to distribution shifts – precisely, the qualities that entropy, PR, and ER quantify. As a result, purely outcome-based metrics cannot explain why certain models generalize better to unforeseen scenarios or why they might fail in settings prioritizing interpretability and robustness, despite strong validation performance. In our study, models with nearly identical accuracy often differed substantially in their latent profiles (Figures 2A vs. 2B), underscoring the orthogonality of extrinsic and intrinsic measures. This finding motivates the development of new evaluations that specifically target the latent traits highlighted by LPP.

LPP-informed tasks for model evaluation

To probe the latent competencies revealed by LPP, we design two diagnostic tasks directly inspired by the intrinsic dynamics of entropy, PR, and ER. The first task, *Ambiguous Reasoning* (AR), presents the model with a prefix containing a lexical ambiguity and then a disambiguating cue, challenging the model to recognize the ambiguity and choose the correct resolution. This task specifically tests the model’s ability to recognize uncertainty and calibrate entropy when resolving ambiguity. The second task, *Symbolic Pattern Completion* (SPC), presents the model with a synthetic sequence governed by a hidden rule (for example, an alternating or mirrored pattern) and requires it to predict the subsequent symbols accurately. This evaluates the model’s capacity for structural compression and pattern generalization, which depend on its representational efficiency (PR and ER). Representative examples of

Metric (symbol)	Mathematical definition	Extremal statistic and interpretation aligned with results
Entropy (H)	$H(x_{\leq t}) = -\sum_v P_{\theta}(v x_{\leq t}) \log P_{\theta}(v x_{\leq t})$, where $P_{\theta}(\cdot x)$ is the next-token distribution	We report: minimum entropy over the rolling-context schedule. <i>Intuition:</i> the entropy floor reflects the lowest uncertainty the model reaches as evidence accumulates. <i>Observed link:</i> higher floors (persistent hesitation) are negatively correlated with extrinsic scores; too-low floors risk overconfident errors.
Effective rank (ER)	Let $C = \text{Cov}(h)$ for hidden states $h = h_{\ell}(x; \theta)$. With singular values $\{\sigma_i\}$ of C and $\tilde{\sigma}_i = \sigma_i / \sum_j \sigma_j$, $ER = \exp\left(-\sum_i \tilde{\sigma}_i \log \tilde{\sigma}_i\right).$	We report: maximum ER across layers and contexts. <i>Intuition:</i> ER estimates representational expansiveness (active dimensionality). <i>Observed link:</i> very high max-ER (over-expanded, weak compression) is negatively correlated with extrinsic scores; moderate ER appears more compatible with strong performance.
Participation ratio (PR)	With eigenvalues $\{\lambda_i\}$ of C , $PR = \frac{(\sum_i \lambda_i)^2}{\sum_i \lambda_i^2}.$	We report: maximum PR across layers and contexts. <i>Intuition:</i> PR reflects how evenly variance is distributed (higher means more diffuse). <i>Observed link:</i> very high max-PR (overly diffuse allocation) is negatively correlated with extrinsic scores; too-low PR risks collapse.

Table 1. Our proposed latent metrics used in LPP. Symbols: $P_{\theta}(v | x)$ is the model next-token distribution; $h_{\ell}(x; \theta)$ are layer- ℓ hidden states; $C = \text{Cov}(h)$; σ_i and λ_i are singular values and eigenvalues of C , respectively. We summarize behavior using extremal statistics (min-entropy, max-ER, max-PR). Our results in Figure 2 show these become negatively correlated with benchmark scores when excessive, indicating harmful uncertainty floors or over-expansive or diffuse representation geometry.

both task types are provided in Table 2. Each task comprises 100 samples and is constructed to avoid training data overlaps, ensuring that performance reflects the model’s intrinsic reasoning abilities rather than memorized knowledge.

Across models, performance on these LPP-informed tasks aligns closely with the models’ latent profiles. In the AR task, models with better-calibrated uncertainty (lower entropy floors) succeed far more often at resolving ambiguities. Accordingly, AR accuracy is strongly *negatively* correlated with minimum entropy across the model pool (Figure 2E); models that maintain low entropy in the face of uncertainty tend to resolve ambiguous prompts correctly, whereas models that exhibit higher irreducible entropy struggle with ambiguity. In the SPC task, we observe a similarly tight link to representational metrics. Models with more compact and less redundant latent representations achieve higher SPC scores, yielding a significant negative correlation between SPC performance and both PR and ER. For example, Mistral-7B, which has one of the most compact latent spaces (low PR and ER), achieves the highest SPC accuracy among the tested models. Notably, Mistral-7B’s strong showing on SPC occurs even though it is not the top performer on any traditional benchmark, highlighting how LPP-based evaluation can surface capabilities that leaderboards miss.

These intrinsic tasks also shed light on model scaling from a process perspective. In general, larger models outperform smaller ones in both AR and SPC, but the improvements are better explained by enhanced latent capabilities than by sheer model size or training data alone. Smaller models in our study tend to be under-confident (higher entropy) and rely on more diffuse activations (higher PR/ER), resulting in lower scores on both tasks. In contrast, the largest models combine low uncertainty with structured, high-dimensional representations, enabling

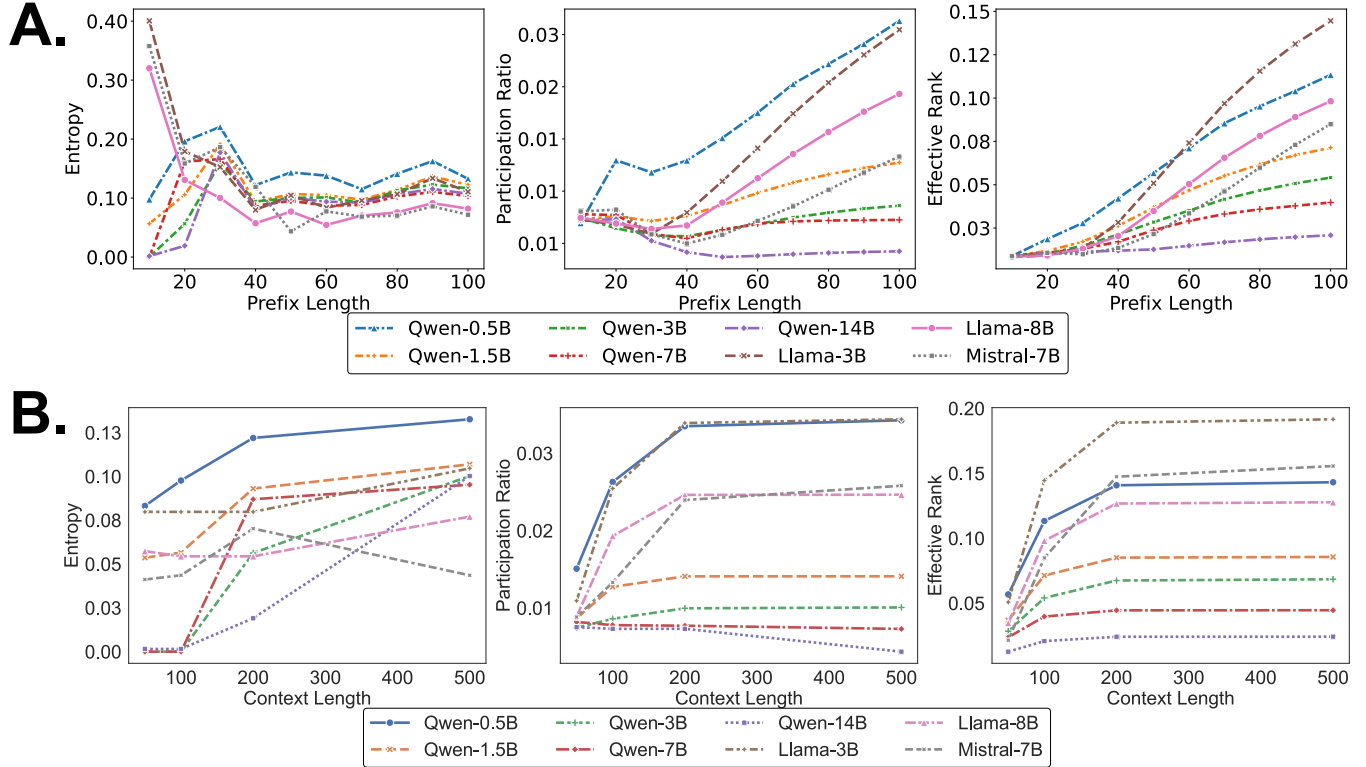


Figure 4. Sensitivity of LPP metrics on (A) prefix length, and (B) context length. Across variations in context and prefix, entropy, participation ratio, and effective rank exhibit smooth and architecture-consistent behavior, establishing them as robust intrinsic indicators of internal model dynamics. Entropy reliably tracks contextual uncertainty, while PR and ER capture representational spread and dimensionality changes with depth and conditioning strength. Notably, increasing context length enriches representation by broadening information integration, whereas longer prefix lengths constrain prediction entropy through stronger conditioning – together revealing complementary yet stable patterns of internal adaptation.

strong performance. Interestingly, AR and SPC performances are largely uncorrelated with each other across models, indicating that each task probes a distinct dimension of latent reasoning (calibration vs. compression). Consistent with this, we find that AR results correlate tightly with entropy-based metrics, whereas SPC results correlate with rank-based metrics (PR, ER), and the cross-correlation between AR-related and SPC-related features is nearly zero. This confirms that the two tasks provide complementary evaluations of model internals.

Crucially, the LPP-guided tasks separate model capabilities more clearly than standard benchmarks. In a two-dimensional plot of AR vs. SPC performance (Figure 3C), models occupy distinct regions corresponding to their latent profiles. Mistral-7B, with its low entropy floor, dominates the AR axis (excelling at ambiguity resolution), whereas Qwen-7B, with an extremely low PR, leads on the SPC axis (excelling at pattern completion). Qwen-14B balances both traits, achieving strong performance on both tasks. This separation is significantly more pronounced than that observed on conventional benchmarks. In fact, models that appear tied in extrinsic accuracy are well-distinguished by their AR and SPC scores, confirming that these tasks capture intrinsic reasoning and representational traits rather than superficial effects of scale. Moreover, because AR and SPC target different latent dimensions, a model’s strengths in one do not guarantee strengths in the other, reinforcing the value of a multifaceted evaluation.

Taken together, our results demonstrate the practical utility of latent profiling. While extrinsic metrics alone cannot predict a model’s reliability on nuanced tasks, LPP exposes latent traits that help explain and even anticipate model behavior. By guiding the design of targeted evaluations (like AR and SPC), LPP offers a path toward more robust benchmarks that probe the mechanisms *underlying* performance rather than merely the end results.

Task	Input	Response
Ambiguous Reasoning (AR)	Consider the ambiguous prefix and two possible senses. First, judge the prefix alone as AMBIGUOUS or NOT AMBIGUOUS. Then, after reading the hint, choose the correct option A or B. Respond strictly as: ambiguous status=AMBIGUOUS or NOT AMBIGUOUS and answer=A or B. Prefix: She deposited money at the, Options: A. bank branch or B. river bank. Hint: The muddy shore was slippery after the rain. Your response:	ambiguous status=AMBIGUOUS; answer=B
Symbolic Pattern Completion (SPC)	You are given a symbolic sequence. Continue it by writing exactly the next 3 symbols, without spaces or explanations. Sequence: DYDYDYDYDYDY Answer:	DYD

Table 2. Examples from LPP-driven synthetic evaluation tasks. This table illustrates two diagnostic task types used in our LPP framework: Ambiguous Reasoning (AR) and Symbolic Pattern Completion (SPC). These tasks are generated to probe specific latent capabilities of LLMs that are not reliably captured by conventional benchmarks. In the AR task, models must resolve lexical ambiguity through contextual inference. The prefix “She deposited money at the” admits two possible continuations – “bank branch” (financial) and “river bank” (geographic). The model must first judge whether the prefix is ambiguous and then resolve it using the disambiguating hint. Success on AR tasks reflects a model’s internal uncertainty modeling and entropy awareness. In contrast, the SPC task evaluates the model’s ability to detect latent symbolic rules and extend them predictively. Given a structured input sequence like DYDYDYDYDYDY, the model must infer the underlying repetition and continue the sequence correctly. These SPC examples are synthetically constructed from rule-based templates (e.g., alternating patterns, mirrored sequences, or modular increments), emphasizing compression and generalization over token memorization. Together, AR and SPC stress-test models on linguistic ambiguity and symbolic abstraction, respectively. Strong performance requires different LPP characteristics: high-entropy awareness for AR, and low participation ratio (PR) and redundancy for SPC.

Discussion

LPP complements traditional benchmarks

Leaderboards provide a convenient snapshot of performance, but our findings show that they can obscure critical facets of model behavior. In our evaluations, models with nearly identical scores on MMLU-PRO, IFEval, or BBH often exhibited very different internal profiles (Figure 2), indicating that high test accuracy can mask underlying vulnerabilities. Indeed, benchmark scores are susceptible to inflation from data overlap, test set memorization, or benchmark-specific fine-tuning, making it difficult to distinguish genuine reasoning ability from exposure-driven artifacts. This issue is exacerbated at scale: large models that differ substantially in calibration, robustness, or representational geometry can nonetheless achieve deceptively similar leaderboard scores. Aggregate metrics collapse diverse behaviors into a single number, hiding failure modes such as miscalibrated uncertainty, brittle intermediate representations, or over-expanded activations that are sensitive to context shifts. Consequently, a high ranking on a public benchmark often provides an incomplete, and sometimes distorted view of a model’s true capabilities. LPP directly addresses these blind spots by quantifying internal properties that conventional benchmarks cannot observe. The entropy, PR, and ER metrics are largely invariant to prompt format or test-set tricks and instead capture stable, intrinsic traits of a model’s computation. By measuring a model’s uncertainty floor, degree of latent compression, and active dimensionality, LPP reveals whether the model’s internal mechanisms are conducive to robust generalization, even when its outward accuracy appears strong.

In our study, we saw that members of the same family (sharing architecture) often exhibit similar LPP signatures even at different scales, whereas models of comparable size from different families can have divergent intrinsic profiles. These nuances are invisible to traditional benchmarks but become clear through LPP analysis. Furthermore, LPP offers an explanation for why extrinsic metrics and latent behavior can diverge: models with similar benchmark scores may rely on entirely different representational strategies, such as compact versus diffuse manifolds, which are not distinguished by accuracy alone. Notably, we also find that model rankings based on LPP metrics are invariant

to the choice of aggregation method (*Supplementary Material* Figure 5 in Section 2.3), whether one uses means, medians, or extremal values, yet different aggregation strategies can highlight distinct aspects of internal behavior. For instance, minimum entropy emphasizes best-case calibration while average PR reflects general representational spread. This suggests that a more informative way to summarize LPP results is through a vectorized profile of multiple statistical summaries per metric, allowing for a richer and more interpretable latent signature. By complementing extrinsic scores with such intrinsic diagnostics, LPP contributes a principled and process-aware layer of model evaluation.

Relation to matrix entropy and interpretability methods

LPP draws conceptual inspiration from earlier work on matrix entropy (Wei et al., 2024) and rank-based evaluations of neural activations (Jha and Reagen, 2025). However, unlike classical matrix entropy measures that are often limited to single snapshots of layer activations or require heuristic normalization, LPP incorporates multiple context lengths and layers to construct a stable latent signature. Moreover, while entropy alone captures the uncertainty in a model’s predictions, it does not reveal how those predictions are supported by internal representations. PR and ER extend beyond this by quantifying the structure and dimensionality of latent spaces, offering a richer picture of how information is stored and transformed. Compared to mechanistic interpretability techniques (Bereska and Gavves, 2024; Dreyer et al., 2025), which aim to dissect individual neurons, attention heads, or circuits, LPP provides a more scalable and model-agnostic diagnostic. Circuit-level approaches can yield powerful insights but often require manual tracing or extensive intervention (e.g., patching or ablation), making them hard to generalize across architectures or tasks. In contrast, LPP requires no supervision or model internals beyond activations, allowing for a systematic comparison across diverse models without requiring task-specific adaptation. It provides coarse-grained but actionable insight into global representational behavior, enabling us to triage which models or layers warrant further mechanistic inspection. Importantly, PR and ER offer distinct advantages over probing-based evaluations. Probing typically focuses on whether particular information (e.g., syntax, world knowledge) is linearly decodable from intermediate representations, which can be misleading: a model may store information in a way that is useful for internal computation but not for external probing. PR and ER sidestep this limitation by measuring the intrinsic geometry of latent spaces, independent of downstream tasks or classifiers. They capture the compressibility and redundancy of activations, properties that directly impact a model’s generalization, efficiency, and susceptibility to adversarial inputs. Thus, LPP augments and extends the existing toolbox of interpretability and diagnostic methods by offering complementary, representation-level insights that are robust, lightweight, and general-purpose.

Stable latent patterns and their origins

Our analyses also shed light on the source of the observed LPP patterns. The entropy, PR, and ER metrics we measured appear to arise from fundamental architectural and representational properties, rather than from idiosyncratic performance differences. In particular, the entropy curves in Figure 4B reveal a consistent early stabilization of uncertainty across all model families. Within just a few tokens of context, each model settles into a characteristic entropy “floor” that remains largely unchanged as additional context is provided. This suggests that a model’s confidence calibration is an intrinsic attribute shaped by its architecture and pre-training dynamics, not something that varies unpredictably with different prompts. In other words, each model has a built-in baseline level of uncertainty it cannot easily reduce, and this level is apparent even in the first few tokens of a prompt.

The representational metrics such as PR and ER exhibit similarly structured behavior. As shown in Figure 4, PR and ER tend to increase smoothly and monotonically with context length for all models. This indicates that as an input sequence grows, models systematically expand the dimensionality of their latent representations, presumably to encode the increasing complexity or information in longer contexts. Notably, this pattern holds across different model families (LLaMA, Qwen, Mistral), hinting at a shared underlying principle of decoder-only transformers: their hidden representations evolve from more compressed manifolds on short prefixes to richer, higher-dimensional subspaces as more context is accumulated. At the same time, different architectures allocate capacity in different ways. For example, Qwen-7B maintains an extremely low PR even at the maximum context length (indicating a very tight, sparse representation), whereas LLaMA-3B’s PR grows much larger, indicating a more diffuse activation pattern. In effect, Qwen-7B aggressively compresses its latent space (perhaps reflecting a more modular or efficient encoding strategy), while LLaMA-3B rapidly expands its latent space, which could make it more expressive but potentially more redundant. Such differences likely stem from architectural choices or training regimes that favor certain encoding strategies over others.

Examining the LPP metrics across model depths further reveals an intriguing “hourglass” structure in how information is processed. We find that entropy, PR, and ER tend to peak near the input embedding layers and

again near the final layers, while the middle layers operate in a more compressed regime (see Figure 4 in Section 2.2 of *Supplementary Materials*). This implies that the models perform an encoder-like expansion of information in the early layers, then distill or compress the information through a bottleneck in the middle layers, and finally re-expand or re-distribute information in the deeper layers before output. Remarkably, we observe this hourglass pattern across models of varying sizes and training data sources, suggesting that it reflects a common computational strategy inherent to the transformer architecture. The consistency of these profiles, along with the context-length trends discussed above, indicates that LPP metrics capture fundamental aspects of model design, such as attention allocation, activation distribution, and the presence of latent bottlenecks. Importantly, we also confirm that these metrics are stable across different datasets, prompt formulations, and sample sizes (see Figure 1–3 in Section 2.1 of *Supplementary Materials*). The robustness of entropy, PR, and ER under such variations supports the view that they measure intrinsic architectural properties rather than artifacts of any particular prompt or dataset. In summary, the latent profiles revealed by LPP appear to originate from the models’ core architecture and training, providing insight into how modern LLMs internally manage information flow and complexity.

Implications for model selection and monitoring

Beyond analysis, LPP offers practical guidance for model selection and deployment. By characterizing models in terms of their latent profiles, we can identify which models are inherently better suited for certain applications. For example, Figure 3B highlights several latent “archetypes.” Models optimized for low entropy (such as Mistral-7B, which achieves the lowest uncertainty floor) may be preferable in settings that require high calibration and caution, such as safety-critical decision-making or handling ambiguous user queries. Low entropy in this context reflects narrower and more confident predictive distributions, which can signal stronger calibration and less epistemic uncertainty (Guo et al., 2017; Ovadia et al., 2019). In safety-critical scenarios, where overconfident yet incorrect outputs can be catastrophic, models with low and stable entropy are better suited, as they are less prone to unpredictable or spurious high-confidence errors. In contrast, models optimized for low PR (such as Qwen-7B, with extremely compact representations) excel at tasks involving algorithmic pattern recognition or symbolic manipulation, where a highly compressed internal representation is beneficial. Meanwhile, a model like Qwen-14B, which balances low entropy and low PR, offers more general-purpose stability, performing reliably across a broad range of tasks. These distinctions are not readily apparent from standard metrics alone, but LPP makes them explicit. Therefore, when choosing an LLM for a particular use case, one can consider its LPP profile (Table 1) in addition to its task accuracy: for instance, preferring a model with a low entropy floor for applications demanding dependable confidence estimates, or a model with a low participation ratio for tasks requiring efficient internal representations.

In deployment, LPP metrics can also serve as valuable monitors for model behavior. Because entropy, PR, and ER respond in predictable ways to increasing context (Figure 4A) and other input perturbations (Figure 4B and *Supplementary Materials*: Figure 1–3 in Section 2.1), deviations from these expected patterns can act as early-warning signals. For example, if a deployed model that normally maintains a certain entropy floor suddenly exhibits a rising entropy trend on incoming data, it may indicate domain drift or novel inputs that undermine the model’s calibration. Similarly, an unexpected spike in effective rank or participation ratio may flag that the model’s internal representations are straying into an anomalously diffuse regime, perhaps due to adversarial inputs or the model entering a corner of its parameter space that is not well-covered during training. Such latent shifts could presage performance degradation or unsafe behavior long before these issues surface in output accuracy. By continuously tracking LPP metrics during inference, practitioners could detect these warning signs and intervene (e.g., by model retraining or input filtering) before failures occur. In this way, LPP enables a form of interpretable model telemetry, providing insight into the model’s “health indicators” in real-time, which supports more stable and accountable deployment. While this work focuses on three core metrics – entropy, participation ratio, and effective rank, the LPP framework is extensible, and future work may introduce additional metrics that target other facets of latent computation such as attention dispersion, context sensitivity, or activation sparsity. Overall, incorporating LPP-based criteria into model selection and monitoring protocols can help ensure that we not only pick models that perform well on paper but also those that exhibit desirable internal behavior during operation.

Materials and Methods

In this section, we formally define the LPP metrics, describe how they are computed, and outline the procedures used for constructing and evaluating synthetic tasks.

Formal definition of LPP metrics

We consider three latent metrics that capture distinct aspects of a model’s internal processing (see Table 1). For a hidden activation tensor $h = h_\ell(x; \theta)$ at layer ℓ and token sequence x , let $C = \text{Cov}(h)$ denote the empirical covariance matrix. Let $\{\lambda_i\}$ and $\{\sigma_i\}$ be the eigenvalues and singular values of C , respectively, and define normalized singular values $\tilde{\sigma}_i = \sigma_i / \sum_j \sigma_j$.

Uncertainty floor (Entropy). For token position t and prefix $x_{\leq t}$, we define next-token entropy as

$$H_t = - \sum_v P_\theta(v | x_{\leq t}) \log P_\theta(v | x_{\leq t}).$$

We track minimum entropy across a rolling-context schedule. A higher entropy floor indicates persistent uncertainty even when contextual cues accumulate, whereas a lower but well-calibrated floor corresponds to models that become confident only when evidence is sufficient. Extremely low floors may signal premature overconfidence.

Representational expansiveness (Effective Rank). With covariance C and singular values $\{\sigma_i\}$, we compute effective rank as

$$\text{ER} = \exp \left(- \sum_i \tilde{\sigma}_i \log \tilde{\sigma}_i \right).$$

ER estimates the number of active dimensions in the hidden representation. Excessively high ER correlates with diffuse, over-expanded representations and degraded task performance, whereas moderate ER reflects rich but structured activity.

Variance distribution (Participation Ratio). Given eigenvalues $\{\lambda_i\}$ of C , we define participation ratio

$$\text{PR} = \frac{(\sum_i \lambda_i)^2}{\sum_i \lambda_i^2}.$$

PR quantifies how evenly variance is distributed across dimensions. A very high PR suggests diffuse activation and redundant capacity allocation, while a lower PR reflects more selective and compressed representations.

To summarize behavior across layers (*Supplementary Material* Figure 4 in Section 2.2) and context lengths (Figure 4), we extract extrema that characterize failure-prone or stability-critical regimes: (i) minimum next-token entropy (entropy floor), (ii) maximum effective rank (max-ER), and (iii) maximum participation ratio (max-PR).

These extrema capture the model’s most confident states and its most expanded or most distributed representational modes. In practice, we compute LPP metrics over 100 Alpaca prompts (Taori et al., 2023), estimate from the last layer of each LLM, and aggregate them using the extrema above to obtain a compact latent profile for each model. We further elaborate on the sensitivity of LPP metrics on different aggregation functions in Figure 5 in Section 2.3 of the *Supplementary Material*.

Implementation details

Models and environment: We evaluate publicly available open-source models from Hugging Face using the `transformers` library. External benchmark scores on MMLU-PRO, BBH, and IFEval are obtained from the Hugging Face leaderboard (Fourrier et al., 2024). For consistent generation across decoder-only models, we use left padding and assign the EOS token as the padding token when it is absent. All experiments set the random seed to 42 for reproducibility, use a batch size of 8 for throughput, and employ greedy decoding (`temperature=0`) for entropy estimation.

Datasets and prompts for intrinsic metrics: Intrinsic metrics are computed using 100 randomly-sampled task-agnostic texts from the Alpaca dataset (Taori et al., 2023). Entropy is evaluated using deterministic decoding (`temperature=0`, `top_p=1.0`) to remove sampling noise; hidden-state metrics use the same forward passes. We use a maximum context length of 200 tokens, with a designated prefix length of 100. Sensitivity analyses vary context length $\{50, 100, 200, 500\}$, prefix length $\{10, 20, 30, 40, 50, 60, 70, 80, 90, 100\}$, and sample size $\{10, 100, 500, 1000\}$ across WikiText (Merity et al., 2017), Dolly (Conover et al., 2023), and Alpaca (Taori et al., 2023). All datasets are English-language corpora for autoregressive generation.

Synthetic tasks motivated by LPP metrics

To probe the latent behaviors revealed by LPP, we construct two synthetic evaluation tasks – Ambiguous Reasoning and Symbolic Pattern Completion, that isolate uncertainty dynamics and representational compression. These tasks are derived directly from the trends observed in entropy, PR, and ER, and avoid contamination by relying on procedurally generated templates. Algorithms 1 and 2 of the *Supplementary Material* Section 1 formalize the synthetic task generation process. Examples provided in Table 2. Each dataset contains 100 samples. **Ambiguous Reasoning (AR):** AR tests whether a model can (i) detect ambiguity in a prefix, and (ii) resolve it after receiving a disambiguating hint. This design operationalizes the uncertainty-floor behavior captured by entropy: models must maintain high entropy before the hint and collapse it appropriately afterward. Prefixes, hints, and answer options are programmatically generated to ensure lexical and semantic variety. **Symbolic Pattern Completion (SPC):** SPC evaluates a model’s ability to infer and extend symbolic rules in short sequences (e.g., alternation, mirroring, modular increments). These tasks reflect compression-based behavior associated with PR and ER: strong models exhibit low PR (selective activation) and moderate ER (sufficient representational richness). Sequences are procedurally generated to avoid domain-specific priors and focus on structural generalization. Both AR and SPC allow precise control over difficulty, sequence structure, and ambiguity type, enabling targeted assessment of the latent dimensions uncovered by LPP.

Evaluating LLMs on the AR and SPC tasks

We evaluate both tasks using few-shot prompting with batched generation. Inputs are left-padded; when no pad token exists for a tokenizer, EOS is substituted to prevent misaligned logits. For AR, we use `max_new_tokens=16`; for SPC, `max_new_tokens=8`. Each model receives 10 in-context examples sampled randomly. **Metrics:** For SPC, we compute character-level F1 and average across samples. For AR, we compute the mean of (i) ambiguity-status accuracy and (ii) answer-choice accuracy. All results are reported as dataset-level averages. Further analyses on the impact of number of in-context examples of the model performance is highlighted in Figure 6 in Section 2.4 of the *Supplementary Material*.

All experiments are conducted on a single Nvidia A100 GPU. Calculating LPP metrics on 100 samples requires 2–4 minutes, depending upon the model sizes.

Data and Code Availability

The source code for reproducing our results is available at <https://github.com/LCS2-IIITD/LPP>. The generated synthetic datasets – AR and SPC are also open-sourced in the same GitHub repository. Extrinsic task performances are obtained from https://huggingface.co/spaces/open-llm-leaderboard/open_llm_leaderboard.

Author Contributions

T.C. perceived the idea. T.C., A.S., S.B., P.P.C., A.C., S.C., P.P.D., L.D., R.S., and M.V. helped in refining the idea. A.S. ran all the experiments. T.C. and A.S. analyzed the results and prepared the initial manuscript. T.C., A.S., S.B., P.P.C., A.C., S.C., P.P.D., L.D., R.S., and M.V. contributed to finalizing the manuscript.

Competing Interests

The authors have no competing interests.

References

- Agrawal, M., Chen, I. Y., Gulamali, F., and Joshi, S. (2025). The evaluation illusion of large language models in medicine. *npj Digital Medicine*, 8(1):600.
- Banerjee, S., Agarwal, A., and Singh, E. (2024). The vulnerability of language model benchmarks: Do they accurately reflect true llm performance? *arXiv preprint arXiv:2412.03597*.
- Bang, Y., Ji, Z., Schelten, A., Hartshorn, A., Fowler, T., Zhang, C., Cancedda, N., and Fung, P. (2025). Hallulens: Llm hallucination benchmark. *arXiv preprint arXiv:2504.17550*.
- Bereska, L. and Gavves, S. (2024). Mechanistic interpretability for AI safety - a review. *Transactions on Machine Learning Research*, pages 1–55.

- Boiko, D. A., MacKnight, R., Kline, B., and Gomes, G. (2023). Autonomous chemical research with large language models. *Nature*, 624(7992):570–578.
- Carranza, J. M. N. (2025). LLMs show surface-form brittleness under paraphrase stress tests. In *NeurIPS 2025 Workshop on Evaluating the Evolving LLM Lifecycle: Benchmarks, Emergent Abilities, and Scaling*, pages 1–5.
- Chang, Y., Wang, X., Wang, J., Wu, Y., Yang, L., Zhu, K., Chen, H., Yi, X., Wang, C., Wang, Y., et al. (2024). A survey on evaluation of large language models. *ACM transactions on intelligent systems and technology*, 15(3):1–45.
- Chen, M. (2021). Evaluating large language models trained on code. *arXiv preprint arXiv:2107.03374*.
- Cobbe, K., Kosaraju, V., Bavarian, M., Chen, M., Jun, H., Kaiser, L., Plappert, M., Tworek, J., Hilton, J., Nakano, R., et al. (2021). Training verifiers to solve math word problems. *arXiv preprint arXiv:2110.14168*.
- Conover, M., Hayes, M., Mathur, A., Xie, J., Wan, J., Shah, S., Ghodsi, A., Wendell, P., Zaharia, M., and Xin, R. (2023). Free dolly: Introducing the world’s first truly open instruction-tuned llm.
- Dohare, S., Hernandez-Garcia, J. F., Lan, Q., Rahman, P., Mahmood, A. R., and Sutton, R. S. (2024). Loss of plasticity in deep continual learning. *Nature*, 632(8026):768–774.
- Dreyer, M., Berend, J., Labarta, T., Vielhaben, J., Wiegand, T., Lapuschkin, S., and Samek, W. (2025). Mechanistic understanding and validation of large AI models with SemanticLens. *Nature Machine Intelligence*, 7(9):1572–1585.
- Dubey, A., Jauhri, A., Pandey, A., Kadian, A., Al-Dahle, A., Letman, A., Mathur, A., Schelten, A., Yang, A., Fan, A., et al. (2024). The llama 3 herd of models. *arXiv preprint arXiv:2407.21783*.
- Farquhar, S., Kossen, J., Kuhn, L., and Gal, Y. (2024). Detecting hallucinations in large language models using semantic entropy. *Nature*, 630(8017):625–630.
- Fodor, J. (2025). Line goes up? inherent limitations of benchmarks for evaluating large language models. *arXiv preprint arXiv:2502.14318*.
- Fourrier, C., Habib, N., Lozovskaya, A., Szafer, K., and Wolf, T. (2024). Open llm leaderboard v2.
- Gilardi, F., Alizadeh, M., and Kubli, M. (2023). Chatgpt outperforms crowd workers for text-annotation tasks. *Proceedings of the National Academy of Sciences*, 120(30):e2305016120.
- Guo, C., Pleiss, G., Sun, Y., and Weinberger, K. Q. (2017). On calibration of modern neural networks. In *Proceedings of the 34th International Conference on Machine Learning - Volume 70, ICML’17*, pages 1321–1330. JMLR.org.
- Guo, J., Gu, S., Jin, M., Spanos, C., and Lavaei, J. (2025). Stylebench: Evaluating thinking styles in large language models. *arXiv preprint arXiv:2509.20868*.
- Haller, P., Ibrahim, M., Kirichenko, P., Sagun, L., and Bell, S. J. (2025). Llm knowledge is brittle: Truthfulness representations rely on superficial resemblance. *arXiv preprint arXiv:2510.11905*.
- Han, J., Kossen, J., Razzak, M., Schut, L., Malik, S. A., and Gal, Y. (2024). Semantic entropy probes: Robust and cheap hallucination detection in llms. In *ICML 2024 Workshop on Foundation Models in the Wild*.
- Hendrycks, D., Burns, C., Basart, S., Zou, A., Mazeika, M., Song, D., and Steinhardt, J. (2021). Measuring massive multitask language understanding. In *International Conference on Learning Representations*, pages 1–27.
- Hernandez, D., Kaplan, J., Henighan, T., and McCandlish, S. (2021). Scaling laws for transfer. *arXiv preprint arXiv:2102.01293*.
- Jha, N. K. and Reagen, B. (2025). Spectral scaling laws in language models: How Effectively Do Feed-Forward Networks Use Their Latent Space? In Christodoulopoulos, C., Chakraborty, T., Rose, C., and Peng, V., editors, *Proceedings of the 2025 Conference on Empirical Methods in Natural Language Processing*, pages 35047–35058, Suzhou, China. Association for Computational Linguistics.
- Jiang, A. Q., Sablayrolles, A., Mensch, A., Bamford, C., Chaplot, D. S., de las Casas, D., Bressand, F., Lengyel, G., Lample, G., Saulnier, L., Lavaud, L. R., Lachaux, M.-A., Stock, P., Scao, T. L., Lavril, T., Wang, T., Lacroix, T., and Sayed, W. E. (2023). Mistral 7b.

- Jiang, A. Q., Sablayrolles, A., Roux, A., Mensch, A., Savary, B., Bamford, C., Chaplot, D. S., Casas, D. d. l., Hanna, E. B., Bressand, F., et al. (2024). Mixtral of experts. *arXiv preprint arXiv:2401.04088*.
- Kaplan, J., McCandlish, S., Henighan, T., Brown, T. B., Chess, B., Child, R., Gray, S., Radford, A., Wu, J., and Amodei, D. (2020). Scaling laws for neural language models. *arXiv preprint arXiv:2001.08361*.
- Li, X., Li, X., Dong, K., Zhang, Q., Ruan, R., Dai, X., Liu, X., Xu, S., Wang, Y., and Tang, R. (2025). Humanity’s last code exam: Can advanced llms conquer human’s hardest code competition? *arXiv preprint arXiv:2506.12713*.
- Liang, P., Bommasani, R., Lee, T., Tsipras, D., Soylu, D., Yasunaga, M., Zhang, Y., Narayanan, D., Wu, Y., Kumar, A., Newman, B., Yuan, B., Yan, B., Zhang, C., Cosgrove, C., Manning, C. D., Re, C., Acosta-Navas, D., Hudson, D. A., Zelikman, E., Durmus, E., Ladhak, F., Rong, F., Ren, H., Yao, H., WANG, J., Santhanam, K., Orr, L., Zheng, L., Yuksekgonul, M., Suzgun, M., Kim, N., Guha, N., Chatterji, N. S., Khattab, O., Henderson, P., Huang, Q., Chi, R. A., Xie, S. M., Santurkar, S., Ganguli, S., Hashimoto, T., Icard, T., Zhang, T., Chaudhary, V., Wang, W., Li, X., Mai, Y., Zhang, Y., and Koreeda, Y. (2023). Holistic evaluation of language models. *Transactions on Machine Learning Research*, pages 1–162.
- Lin, B. Y., Deng, Y., Chandu, K., Ravichander, A., Pyatkin, V., Dziri, N., Bras, R. L., and Choi, Y. (2025). Wildbench: Benchmarking LLMs with challenging tasks from real users in the wild. In *The Thirteenth International Conference on Learning Representations*, pages 1–19.
- Lin, S., Hilton, J., and Evans, O. (2022). TruthfulQA: Measuring how models mimic human falsehoods. In Muresan, S., Nakov, P., and Villavicencio, A., editors, *Proceedings of the 60th Annual Meeting of the Association for Computational Linguistics (Volume 1: Long Papers)*, pages 3214–3252, Dublin, Ireland. Association for Computational Linguistics.
- Merity, S., Xiong, C., Bradbury, J., and Socher, R. (2017). Pointer sentinel mixture models. In *International Conference on Learning Representations*, pages 1–15.
- Meta, A. (2025). The llama 4 herd: The beginning of a new era of natively multimodal ai innovation. <https://ai.meta.com/blog/llama-4-multimodal-intelligence/>, checked on, 4(7):2025.
- Milano, S., McGrane, J. A., and Leonelli, S. (2023). Large language models challenge the future of higher education. *Nature Machine Intelligence*, 5(4):333–334.
- Miret, S. and Krishnan, N. M. A. (2025). Enabling large language models for real-world materials discovery. *Nature Machine Intelligence*, 7(7):991–998.
- Muralidharan, S., Turuvekere Sreenivas, S., Joshi, R., Chochowski, M., Patwary, M., Shoeybi, M., Catanzaro, B., Kautz, J., and Molchanov, P. (2024). Compact language models via pruning and knowledge distillation. *Advances in Neural Information Processing Systems*, 37:41076–41102.
- Ovadia, Y., Fertig, E., Ren, J., Nado, Z., Sculley, D., Nowozin, S., Dillon, J., Lakshminarayanan, B., and Snoek, J. (2019). Can you trust your model’s uncertainty? evaluating predictive uncertainty under dataset shift. In Wallach, H., Larochelle, H., Beygelzimer, A., d’Alché-Buc, F., Fox, E., and Garnett, R., editors, *Advances in Neural Information Processing Systems*, volume 32, pages 1–12. Curran Associates, Inc.
- Patil, S. G., Mao, H., Yan, F., Ji, C. C.-J., Suresh, V., Stoica, I., and Gonzalez, J. E. (2025). The berkeley function calling leaderboard (BFCL): From tool use to agentic evaluation of large language models. In *Forty-second International Conference on Machine Learning*, pages 1–22.
- Sainz, O., Campos, J., García-Ferrero, I., Etxaniz, J., de Lacalle, O. L., and Agirre, E. (2023). NLP evaluation in trouble: On the need to measure LLM data contamination for each benchmark. In Bouamor, H., Pino, J., and Bali, K., editors, *Findings of the Association for Computational Linguistics: EMNLP 2023*, pages 10776–10787, Singapore. Association for Computational Linguistics.
- Sharma, A. and Chopra, P. (2025). Think just enough: Sequence-level entropy as a confidence signal for llm reasoning. *arXiv preprint arXiv:2510.08146*.
- Skean, O., Arefin, M. R., Zhao, D., Patel, N. N., Naghiyev, J., LeCun, Y., and Shwartz-Ziv, R. (2025). Layer by layer: Uncovering hidden representations in language models. In *Forty-second International Conference on Machine Learning*, pages 1–22.

Srivastava, A., Rastogi, A., Rao, A., Shoeb, A. A. M., Abid, A., Fisch, A., Brown, A. R., Santoro, A., Gupta, A., Garriga-Alonso, A., Kluska, A., Lewkowycz, A., Agarwal, A., Power, A., Ray, A., Warstadt, A., Kocurek, A. W., Safaya, A., Tazarv, A., Xiang, A., Parrish, A., Nie, A., Hussain, A., Askell, A., Dsouza, A., Slone, A., Rahane, A., Iyer, A. S., Andreassen, A. J., Madotto, A., Santilli, A., Stuhlmüller, A., Dai, A. M., La, A., Lampinen, A. K., Zou, A., Jiang, A., Chen, A., Vuong, A., Gupta, A., Gottardi, A., Norelli, A., Venkatesh, A., Gholamidavoodi, A., Tabassum, A., Menezes, A., Kirubarajan, A., Mullokandov, A., Sabharwal, A., Herrick, A., Efrat, A., Erdem, A., Karakaş, A., Roberts, B. R., Loe, B. S., Zoph, B., Bojanowski, B., Özyurt, B., Hedayatnia, B., Neyshabur, B., Inden, B., Stein, B., Ekmekci, B., Lin, B. Y., Howald, B., Orinon, B., Diao, C., Dour, C., Stinson, C., Argueta, C., Ferri, C., Singh, C., Rathkopf, C., Meng, C., Baral, C., Wu, C., Callison-Burch, C., Waites, C., Voigt, C., Manning, C. D., Potts, C., Ramirez, C., Rivera, C. E., Siro, C., Raffel, C., Ashcraft, C., Garbacea, C., Sileo, D., Garrette, D., Hendrycks, D., Kilman, D., Roth, D., Freeman, C. D., Khashabi, D., Levy, D., González, D. M., Perszyk, D., Hernandez, D., Chen, D., Ippolito, D., Gilboa, D., Dohan, D., Drakard, D., Jurgens, D., Datta, D., Ganguli, D., Emelin, D., Kleyko, D., Yuret, D., Chen, D., Tam, D., Hupkes, D., Misra, D., Buzan, D., Molloy, D. C., Yang, D., Lee, D.-H., Schrader, D., Shutova, E., Cubuk, E. D., Segal, E., Hagerman, E., Barnes, E., Donoway, E., Pavlick, E., Rodolà, E., Lam, E., Chu, E., Tang, E., Erdem, E., Chang, E., Chi, E. A., Dyer, E., Jerzak, E., Kim, E., Manyasi, E. E., Zheltonozhskii, E., Xia, F., Siar, F., Martínez-Plumed, F., Happé, F., Chollet, F., Rong, F., Mishra, G., Winata, G. I., de Melo, G., Kruszewski, G., Parascandolo, G., Mariani, G., Wang, G. X., Jaimovitch-Lopez, G., Betz, G., Gur-Ari, G., Galijasevic, H., Kim, H., Rashkin, H., Hajishirzi, H., Mehta, H., Bogar, H., Shevlin, H. F. A., Schuetze, H., Yakura, H., Zhang, H., Wong, H. M., Ng, I., Noble, I., Jumelet, J., Geissinger, J., Kernion, J., Hilton, J., Lee, J., Fisac, J. F., Simon, J. B., Koppel, J., Zheng, J., Zou, J., Kocon, J., Thompson, J., Wingfield, J., Kaplan, J., Radom, J., Sohl-Dickstein, J., Phang, J., Wei, J., Yosinski, J., Novikova, J., Bosscher, J., Marsh, J., Kim, J., Taal, J., Engel, J., Alabi, J., Xu, J., Song, J., Tang, J., Waweru, J., Burden, J., Miller, J., Balis, J. U., Batchelder, J., Berant, J., Frohberg, J., Rozen, J., Hernandez-Orallo, J., Boudeman, J., Guerr, J., Jones, J., Tenenbaum, J. B., Rule, J. S., Chua, J., Kanclerz, K., Livescu, K., Krauth, K., Gopalakrishnan, K., Ignatyeva, K., Markert, K., Dhole, K., Gimpel, K., Omondi, K., Mathewson, K. W., Chiafullo, K., Shkaruta, K., Shridhar, K., McDonell, K., Richardson, K., Reynolds, L., Gao, L., Zhang, L., Dugan, L., Qin, L., Contreras-Ochando, L., Morency, L.-P., Moschella, L., Lam, L., Noble, L., Schmidt, L., He, L., Oliveros-Colón, L., Metz, L., Senel, L. K., Bosma, M., Sap, M., Hovee, M. T., Farooqi, M., Faruqui, M., Mazeika, M., Baturan, M., Marelli, M., Maru, M., Ramirez-Quintana, M. J., Tolkiehn, M., Giulianelli, M., Lewis, M., Potthast, M., Leavitt, M. L., Hagen, M., Schubert, M., Baitemirova, M. O., Arnaud, M., McElrath, M., Yee, M. A., Cohen, M., Gu, M., Ivanitskiy, M., Starritt, M., Strube, M., Swędrowski, M., Bevilacqua, M., Yasunaga, M., Kale, M., Cain, M., Xu, M., Suzgun, M., Walker, M., Tiwari, M., Bansal, M., Aminnaseri, M., Geva, M., Gheini, M., T, M. V., Peng, N., Chi, N. A., Lee, N., Krakover, N. G.-A., Cameron, N., Roberts, N., Doiron, N., Martinez, N., Nangia, N., Deckers, N., Muennighoff, N., Keskar, N. S., Iyer, N. S., Constant, N., Fiedel, N., Wen, N., Zhang, O., Agha, O., Elbaghdadi, O., Levy, O., Evans, O., Casares, P. A. M., Doshi, P., Fung, P., Liang, P. P., Vicol, P., Alipoormolabashi, P., Liao, P., Liang, P., Chang, P. W., Eckersley, P., Htut, P. M., Hwang, P., Miłkowski, P., Patil, P., Pezheshkpour, P., Oli, P., Mei, Q., Lyu, Q., Chen, Q., Banjade, R., Rudolph, R. E., Gabriel, R., Habacker, R., Risco, R., Millière, R., Garg, R., Barnes, R., Saurous, R. A., Arakawa, R., Raymaekers, R., Frank, R., Sikand, R., Novak, R., Sitelew, R., Bras, R. L., Liu, R., Jacobs, R., Zhang, R., Salakhutdinov, R., Chi, R. A., Lee, S. R., Stovall, R., Teehan, R., Yang, R., Singh, S., Mohammad, S. M., Anand, S., Dillavou, S., Shleifer, S., Wiseman, S., Gruetter, S., Bowman, S. R., Schoenholz, S. S., Han, S., Kwatra, S., Rous, S. A., Ghazarian, S., Ghosh, S., Casey, S., Bischoff, S., Gehrmann, S., Schuster, S., Sadeghi, S., Hamdan, S., Zhou, S., Srivastava, S., Shi, S., Singh, S., Asaadi, S., Gu, S. S., Pachchigar, S., Toshniwal, S., Upadhyay, S., Debnath, S. S., Shakeri, S., Thormeyer, S., Melzi, S., Reddy, S., Makini, S. P., Lee, S.-H., Torene, S., Hatwar, S., Dehaene, S., Divic, S., Ermon, S., Biderman, S., Lin, S., Prasad, S., Piantadosi, S., Shieber, S., Misherghi, S., Kiritchenko, S., Mishra, S., Linzen, T., Schuster, T., Li, T., Yu, T., Ali, T., Hashimoto, T., Wu, T.-L., Desbordes, T., Rothschild, T., Phan, T., Wang, T., Nkinyili, T., Schick, T., Kornev, T., Tunduny, T., Gerstenberg, T., Chang, T., Neeraj, T., Khot, T., Shultz, T., Shaham, U., Misra, V., Demberg, V., Nyamai, V., Raunak, V., Ramasesh, V. V., vinay uday prabhu, Padmakumar, V., Srikumar, V., Fedus, W., Saunders, W., Zhang, W., Vossen, W., Ren, X., Tong, X., Zhao, X., Wu, X., Shen, X., Yaghoobzadeh, Y., Lakretz, Y., Song, Y., Bahri, Y., Choi, Y., Yang, Y., Hao, S., Chen, Y., Belinkov, Y., Hou, Y., Hou, Y., Bai, Y., Seid, Z., Zhao, Z., Wang, Z., Wang, Z. J., Wang, Z., and Wu, Z. (2023). Beyond the imitation game: Quantifying and extrapolating the capabilities of language models. *Transactions on Machine Learning Research*, pages 1–95.

Steyvers, M., Tejada, H., Kumar, A., Belem, C., Karny, S., Hu, X., Mayer, L. W., and Smyth, P. (2025). What large language models know and what people think they know. *Nature Machine Intelligence*, 7(2):221–231.

- Taori, R., Gulrajani, I., Zhang, T., Dubois, Y., Li, X., Guestrin, C., Liang, P., and Hashimoto, T. B. (2023). Stanford alpaca: An instruction-following llama model. *GitHub repository*.
- Wang, Y., Ma, X., Zhang, G., Ni, Y., Chandra, A., Guo, S., Ren, W., Arulraj, A., He, X., Jiang, Z., Li, T., Ku, M., Wang, K., Zhuang, A., Fan, R., Yue, X., and Chen, W. (2024). Mmlu-pro: A more robust and challenging multi-task language understanding benchmark. In Globerson, A., Mackey, L., Belgrave, D., Fan, A., Paquet, U., Tomczak, J., and Zhang, C., editors, *Advances in Neural Information Processing Systems*, volume 37, pages 95266–95290. Curran Associates, Inc.
- Wei, L., Tan, Z., Li, C., Wang, J., and Huang, W. (2024). Diff-erank: A novel rank-based metric for evaluating large language models. *Advances in Neural Information Processing Systems*, 37:39501–39521.
- Xin, H., Kitchin, J. R., and Kulik, H. J. (2025). Towards agentic science for advancing scientific discovery. *Nature Machine Intelligence*, 7(9):1373–1375.
- Yang, A., Li, A., Yang, B., Zhang, B., Hui, B., Zheng, B., Yu, B., Gao, C., Huang, C., Lv, C., et al. (2025). Qwen3 technical report. *arXiv preprint arXiv:2505.09388*.
- Zhao, Q., Huang, Y., Lv, T., Cui, L., Sun, Q., Mao, S., Zhang, X., Xin, Y., Yin, Q., Li, S., and Wei, F. (2025). MMLU-CF: A contamination-free multi-task language understanding benchmark. In Che, W., Nabende, J., Shutova, E., and Pilehvar, M. T., editors, *Proceedings of the 63rd Annual Meeting of the Association for Computational Linguistics (Volume 1: Long Papers)*, pages 13371–13391, Vienna, Austria. Association for Computational Linguistics.
- Zhou, J., Lu, T., Mishra, S., Brahma, S., Basu, S., Luan, Y., Zhou, D., and Hou, L. (2023). Instruction-following evaluation for large language models. *arXiv preprint arXiv:2311.07911*.
- Zhou, L., Schellaert, W., Martínez-Plumed, F., Moros-Daval, Y., Ferri, C., and Hernández-Orallo, J. (2024). Larger and more instructable language models become less reliable. *Nature*, 634(8032):61–68.
- Zhuang, R., Wu, T., Wen, Z., Li, A., Jiao, J., and Ramchandran, K. (2025). EmbedLLM: Learning compact representations of large language models. In *The Thirteenth International Conference on Learning Representations*, pages 1–14.
- Zhuo, T. Y., Chien, V. M., Chim, J., Hu, H., Yu, W., Widyasari, R., Yusuf, I. N. B., Zhan, H., He, J., Paul, I., Brunner, S., GONG, C., Hoang, J., Zebaze, A. R., Hong, X., Li, W.-D., Kaddour, J., Xu, M., Zhang, Z., Yadav, P., Jain, N., Gu, A., Cheng, Z., Liu, J., Liu, Q., Wang, Z., Lo, D., Hui, B., Muennighoff, N., Fried, D., Du, X., de Vries, H., and Werra, L. V. (2025). Bigcodebench: Benchmarking code generation with diverse function calls and complex instructions. In *The Thirteenth International Conference on Learning Representations*, pages 1–55.

Supplementary Material

1 Materials and Methods

1.1 Generation of synthetic tasks

To evaluate how intrinsic latent properties of LLMs relate to their reasoning capabilities, we design two synthetic diagnostic tasks: Ambiguous Reasoning (AR) and Symbolic Pattern Completion (SPC). These tasks are explicitly constructed to probe the uncertainty calibration and representational compactness of language models, guided by LPP metrics such as entropy, effective rank (ER), and participation ratio (PR).

1.1.1 Ambiguous Reasoning (AR)

The AR task is designed to assess a model’s ability to resolve contextual ambiguity in uncertain situations. It requires the model to choose between two plausible interpretations of a prefix, with only a subtle hint provided for disambiguation. Task generation follows these steps:

- We begin with natural text prompts drawn from curated corpora such as Alpaca (Taori et al., 2023) or open-source instruction datasets.
- Prefixes are truncated to a fixed length (e.g., 30 tokens) and evaluated for predictive entropy using the target LLM. Prefixes with high entropy, indicating low model certainty, are selected.
- For each prefix, two plausible completions are curated: one is contextually coherent given a subtle semantic cue, while the other is a foil completion that would appear valid in the absence of deeper reasoning.
- A minimal hint is injected - often a factual or logical constraint, that disambiguates the correct choice.
- The model is asked to choose the correct option (A or B) based on the prefix and hint.

By design, solving AR tasks depends on internal entropy calibration. Well-calibrated models are expected to exhibit lower entropy and improved selection accuracy.

Algorithm 1 Generate AR Tasks Guided by LPP Metrics

```
1: Input: Unambiguous corpus  $\mathcal{C}$ , prefix length  $L_p$ , hint templates  $\mathcal{H}$ , target LPP threshold (high entropy)
2: Output: Ambiguous Reasoning task set  $\mathcal{T}_{AR}$ 
3: Initialize task set  $\mathcal{T}_{AR} \leftarrow \emptyset$ 
4: for all sentence  $s$  in  $\mathcal{C}$  do
5:   Extract prefix  $p = s[:L_p]$ 
6:   Compute entropy  $H(p)$  using LLM predictive distribution
7:   if  $H(p) >$  entropy threshold then
8:     Identify two plausible suffix interpretations  $s_1, s_2$ 
9:     Generate hint  $h \sim \mathcal{H}$  to disambiguate between  $s_1, s_2$ 
10:    Format input prompt:
11:    Prefix:  $p$ , Options: A.  $s_1$ , B.  $s_2$ , Hint:  $h$ 
12:    Append to  $\mathcal{T}_{AR}$  with correct disambiguated answer
13:   end if
14: end for
15: return  $\mathcal{T}_{AR}$ 
```

1.1.2 Symbolic Pattern Completion (SPC)

The SPC task probes whether models can extract, compress, and generalize symbolic rules, emulating a low-dimensional representation strategy. It is constructed as follows:

- A library of symbolic patterns is defined over a limited alphabet (e.g., A, B, C, D). Patterns include alternation (e.g., ABAB), mirroring (e.g., ABBA), progression (e.g., ABCD), or nested rules.
- For each pattern, sequences of a fixed length (e.g., 12 tokens) are generated, ensuring that a predictable rule governs the structure.

- The final few tokens are masked, and the model is tasked with completing the sequence.
- The correct completions require internalizing the latent rule and generating the expected continuation.

SPC performance is hypothesized to correlate with representational compactness, specifically low effective rank and participation ratio. Models with highly distributed representations may overfit the surface form, while models with tight low-rank activations are better positioned to abstract and generalize.

Algorithm 2 Generate SPC Tasks Guided by LPP Metrics

- 1: **Input:** Symbol set Σ , template library \mathcal{P} (e.g., alternation, mirroring), desired sequence length L , target LPP profile (low PR/ER)
 - 2: **Output:** Symbolic Pattern Completion task set \mathcal{T}_{SPC}
 - 3: Initialize task set $\mathcal{T}_{SPC} \leftarrow \emptyset$
 - 4: **for all** pattern P in \mathcal{P} **do**
 - 5: Sample symbols $\{s_i\} \subseteq \Sigma$
 - 6: Generate sequence $S = P(s_1, \dots, s_k)$ of length L
 - 7: Select a prefix $S_{\text{prefix}} = S[:L-3]$, target completion $S_{\text{suffix}} = S[L-3:]$
 - 8: Format input prompt:
 Sequence: S_{prefix} , **Answer:** S_{suffix}
 - 9: Append to \mathcal{T}_{SPC}
 - 10: **end for**
 - 11: **return** \mathcal{T}_{SPC}
-

1.2 Extrinsic benchmarks

MMLU-Pro. MMLU-Pro (Wang et al., 2024) is an enhanced multi-task language understanding benchmark designed to address limitations of the original MMLU (Hendrycks et al., 2021) by incorporating more challenging reasoning problems and reducing trivial or flawed questions. It consists of over 12,000 multiple-choice questions spanning 14 diverse domains such as mathematics, physics, law, and health, primarily targeting college-level difficulty. Each question includes ten answer options, compared to four in the original MMLU and thereby increasing the difficulty and reducing the impact of random guessing. The benchmark emphasizes multi-step reasoning and complex problem solving, and models generally benefit from chain-of-thought prompting rather than direct answering. Questions have been thoroughly curated and validated to ensure clarity and correctness, resulting in more reliable and interpretable evaluations. Top-performing models still fall short of perfect accuracy, making MMLU-Pro a valuable tool for measuring both knowledge and reasoning proficiency in large language models.

IFEval. IFEval (Zhou et al., 2023) is a benchmark designed to evaluate an LLM’s ability to follow explicit instructions. Unlike traditional question-answering datasets, IFEval focuses on compliance with verifiable directives – such as generating text with a certain number of words, including specific keywords, or formatting content in a particular way. It comprises 500 instruction-rich prompts, each embedding one or more of 25 requirement types. The responses are evaluated using deterministic programmatic checks, allowing objective, reproducible measurement of how well a model follows instructions. Metrics include prompt-level strict accuracy and instruction-level accuracy, reflecting whether all or individual requirements are satisfied. IFEval isolates the dimension of instruction adherence, providing critical insight into how reliably a model follows user intent, especially relevant for safety-sensitive and user-facing deployments.

BIG-Bench Hard (BBH). BBH (Zhuo et al., 2025) is a curated subset of 23 tasks from the broader BIG-Bench suite, selected because they proved difficult for prior models to solve. These tasks cover a wide array of domains, including logic, mathematics, commonsense reasoning, and creative problem-solving, and are designed to stress-test a model’s reasoning capabilities. BBH tasks generally require multi-step inference, compositional thinking, or the ability to follow complex chains of logic. Chain-of-thought prompting significantly improves performance on BBH, revealing deeper reasoning capabilities in modern LLMs that are not evident under standard prompting. By focusing on tasks that challenge reasoning depth rather than surface-level knowledge, BBH serves as a diagnostic benchmark for assessing emergent problem-solving abilities in large language models.

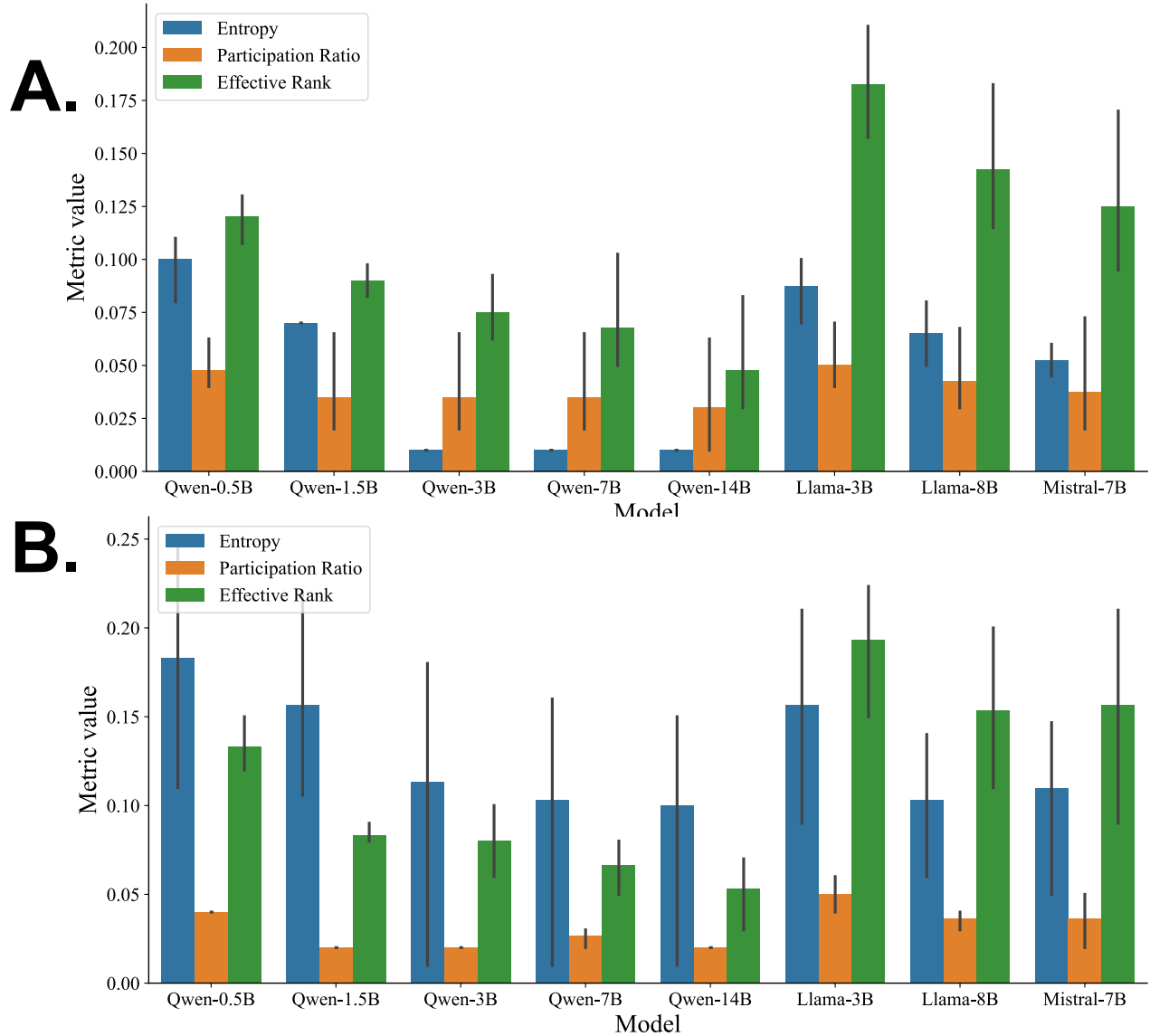


Figure 1. Sensitivity of intrinsic metrics across sample size (A) and dataset (B). We use dataset sample sizes of $\{10, 100, 500, 1000\}$ and three different language modeling datasets – Alpaca, Dolly, and WikiText. Detailed results shown in Figures 2 and 3, respectively. Each bar shows the mean entropy, PR, and ER across models and datasets. The trends demonstrate that while dataset-specific scaling slightly shifts the absolute metric values, the relative ordering and inter-metric consistency remain stable – highlighting that entropy, PR, and ER act as robust, dataset-invariant indicators of internal representational dynamics.

2 Additional results and discussion

2.1 Sensitivity of LPP metrics across sample sizes, datasets

We investigate the robustness of LPP metrics – entropy, PR, and ER with respect to different sample sizes and calibration datasets. Figure 1 provides a comprehensive view of how these metrics vary under such changes.

Sample Size Sensitivity. In Figure 1A (details in Figure 2), we compute entropy, PR, and ER across different models using the Alpaca dataset at four different sample sizes: 10, 100, 500, and 1000. Across all models and metrics, we observe that the values stabilize quickly with increasing sample size. Entropy estimates show a slight upward shift from 10 to 100 samples but plateau beyond that, suggesting early convergence. PR and ER values similarly show

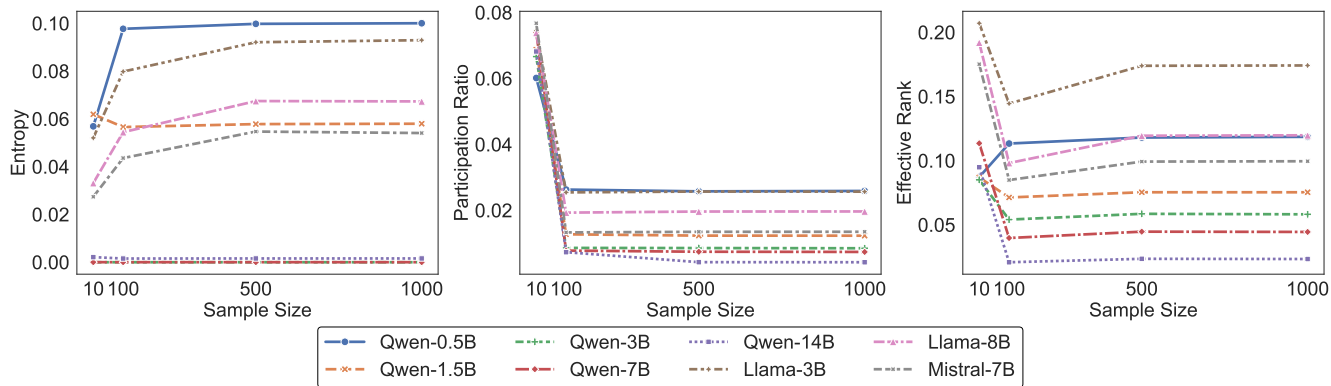


Figure 2. Stability of LPP metrics across varying sample sizes. This figure presents entropy (left), participation ratio (center), and effective rank (right) computed over increasing sample sizes (10, 100, 500, 1000) from the Alpaca dataset for different LLMs. Each line denotes a different model. Entropy values (left) increase and then stabilize for all models, indicating early convergence in output uncertainty. The participation ratio (middle) and effective rank (right) exhibit sharp initial changes at small sample sizes (from 10 to 100), but quickly plateau thereafter, underscoring the robustness of representational metrics. Across all metrics, model ranking remains largely unchanged with larger sample sizes, reflecting that these metrics capture stable, architecture-dependent properties rather than dataset-specific noise. These findings confirm that reliable estimation of intrinsic model characteristics via LPP can be achieved with relatively modest calibration data sizes.

minor fluctuations between 10 and 100 samples but become virtually invariant as sample size increases to 500 and 1000. This stability suggests that LPP metrics are highly sample-efficient, allowing for reliable estimates of latent model behavior to be computed using as few as 100 samples. Additionally, the relative ordering of models by entropy, PR, and ER remains largely unchanged across sample sizes, confirming that the LPP metrics capture consistent latent traits.

Dataset Sensitivity. In Figure 1B (details in Figure 3), we compute the same metrics across three different datasets – Alpaca (Taori et al., 2023), Dolly (Conover et al., 2023), and WikiText (Merity et al., 2017), while keeping the sample size fixed at 100. We find that absolute values of entropy, PR, and ER differ slightly across datasets, with WikiText generally producing higher entropy and lower PR. However, the relative model rankings remain stable across all datasets. For example, Qwen-14B consistently maintains lower PR and ER across all three corpora, while LLaMA-8B and LLaMA-3B show higher entropy and effective rank. This consistency suggests that LPP metrics are dataset-agnostic to a useful extent, meaning they are not strongly influenced by prompt style, task format, or lexical diversity.

2.2 Layerwise Analysis of LPP Metrics

We further analyze the distribution of latent metrics across different layers of each model. Figure 4 shows the PR and ER values as functions of normalized layer depth, ranging from input (0.0) to output (1.0). Entropy is calculated based on the probability of the next token; therefore, it does not depend on the model layers and is omitted from this analysis.

Hourglass Structure. All models exhibit a pronounced “hourglass” shape in their layer-wise profiles. PR and ER values are highest at the initial embedding and early transformer blocks, decrease significantly in mid-layers, and rise again toward the output layers. This pattern suggests that the representational space is initially high-dimensional and expansive, but compressed into a low-dimensional subspace during intermediate processing, and remains high-dimensional and expansive at the beginning and end of the model. This compression-expansion pattern suggests an encoder-like structure within decoder-only architectures: initial layers expand raw inputs into a diverse representation; middle layers distill this into abstract, compact signals; and final layers re-expand these into expressive distributions over output tokens.

Consistency Across Models. Importantly, this hourglass pattern is consistent across model sizes and families. All models follow the same trajectory despite differences in depth, architecture, and training corpus. Larger models tend to have deeper hourglass dips (more compression) and higher expansion at the boundaries, consistent with

their increased capacity. This universal structure implies that LPP metrics reveal fundamental, architecture-driven processing stages that reflect how transformer LLMs manage information internally.

2.3 Influence of Aggregation Method on LPP Ranking

A critical consideration in the application of LPP lies in the choice of aggregation function used to summarize metric values across input samples. Since entropy, PR, and ER are each computed per input instance, aggregating these into a single model-level summary necessitates design choices that can significantly influence the final ranking. Figure 5 presents a comparative analysis of five aggregation strategies applied to LPP metrics. Our original formulation (Figure 5a), adopts *minimum* entropy to capture the most confident state of the model, while using *maximum* values for PR and ER to represent peak representational spread and dimensionality. This combination emphasizes worst-case overconfidence and best-case expressivity. However, alternative aggregation schemes offer competing interpretations. Median-based aggregation (Figure 5b) dampens the influence of outliers, producing smoother profiles. Mean-based summaries (Figure 5c) provide a central tendency, yet risk being skewed by extreme values. Minimum aggregation (Figure 5d) across all metrics, thus favoring the most conservative estimation of representational complexity. Conversely, Figure 5e emphasizes the *maximum* values across all metrics, amplifying the most expressive model states.

Despite overall consistency in model rankings – e.g., Mistral-7B and Qwen-14B maintaining superior scores across most variants—the relative prominence of other models such as Llama-3B or Qwen-3B fluctuates depending on the chosen scheme. This underscores that LPP rankings are sensitive to aggregation strategy, and that interpretations drawn from latent metrics must be accompanied by transparent reporting of the summarization method used.

In conclusion, our findings highlight that while LPP is robust in capturing intrinsic model traits, comparative profiling remains contingent on different aggregation methods. For meaningful and reproducible model diagnostics, especially when ranking models based on latent behavior, the choice of aggregation must be explicitly justified and standardized where possible.

2.4 In-context performance of LLMs on synthetic tasks

To assess how LLMs leverage context, we evaluated their performance on AR and SPC tasks across varying numbers of in-context examples ($k \in \{0, 1, 5, 10\}$). Figure 6 illustrates the accuracy and F1 score results obtained on AR and SPC, respectively. A consistent upward trend emerges for most models, where performance improves with the number of in-context examples. This effect is especially pronounced for larger models such as Qwen-14B and Mistral-7B. For example, Mistral-7B achieves near-saturating performance with just five to ten examples, highlighting its capacity for effective few-shot learning. Qwen-14B follows a similar pattern, benefiting notably from increased context, especially on the SPC task. In contrast, smaller models, such as Qwen-0.5B and Qwen-1.5B, exhibit only marginal improvements as k increases, underscoring their limited ability to utilize in-context signals. These results emphasize the role of model capacity in enabling in-context generalization, with more expressive models demonstrating superior adaptability to additional contextual cues.

2.5 Future directions for intrinsic profiling

The LPP framework lays a foundation for expanding intrinsic evaluation beyond the three metrics explored in this study. Our robustness experiments (Figure 1) hint that additional latent metrics could be developed to capture other facets of internal model dynamics. For instance, one could measure *representational modularity* (how discretely clustered the activation space is), *perturbation sensitivity* (how small input changes affect internal states) or *latent stability* under various input transformations. These metrics might reveal aspects of model reasoning and structure – such as the degree of compartmentalization of knowledge or the resilience of internal circuits – that complement entropy, PR, and ER. Another promising avenue is to incorporate LPP principles into training objectives. By regularizing models toward desirable latent profiles (for example, penalizing overly high participation ratios or encouraging a well-calibrated entropy floor), we can prevent pathological behaviors such as collapsed representations or erratic confidence spikes during learning. Such *LPP-aware training* could align model geometry with robust generalization from the outset, rather than only diagnosing problems post hoc.

Extending intrinsic profiling to new model classes is an important next step. Thus far, we have focused on decoder-only language models; however, the same philosophy can be applied to multimodal models, memory-augmented architectures, or agentic systems that interact with environments. Each of these introduces additional complexity – for example, vision-language models might require metrics for cross-modal alignment, and agent models might need metrics for planning or state representation. Investigating whether the geometric principles observed in LLMs (like the hourglass compression pattern or entropy stabilization) hold in these other domains will be illuminating. It may turn out that entirely new intrinsic metrics are needed to capture their unique behaviors. As AI

systems continue to scale in size and complexity, purely extrinsic evaluation will become increasingly inadequate for ensuring reliability. LPP offers a principled pathway toward more interpretable, reliable, and diagnostically transparent model evaluation. By enriching our toolkit with intrinsic metrics and tasks, we can gain a deeper understanding of model internals and build confidence that our models are not just performing well, but doing so for the right reasons.

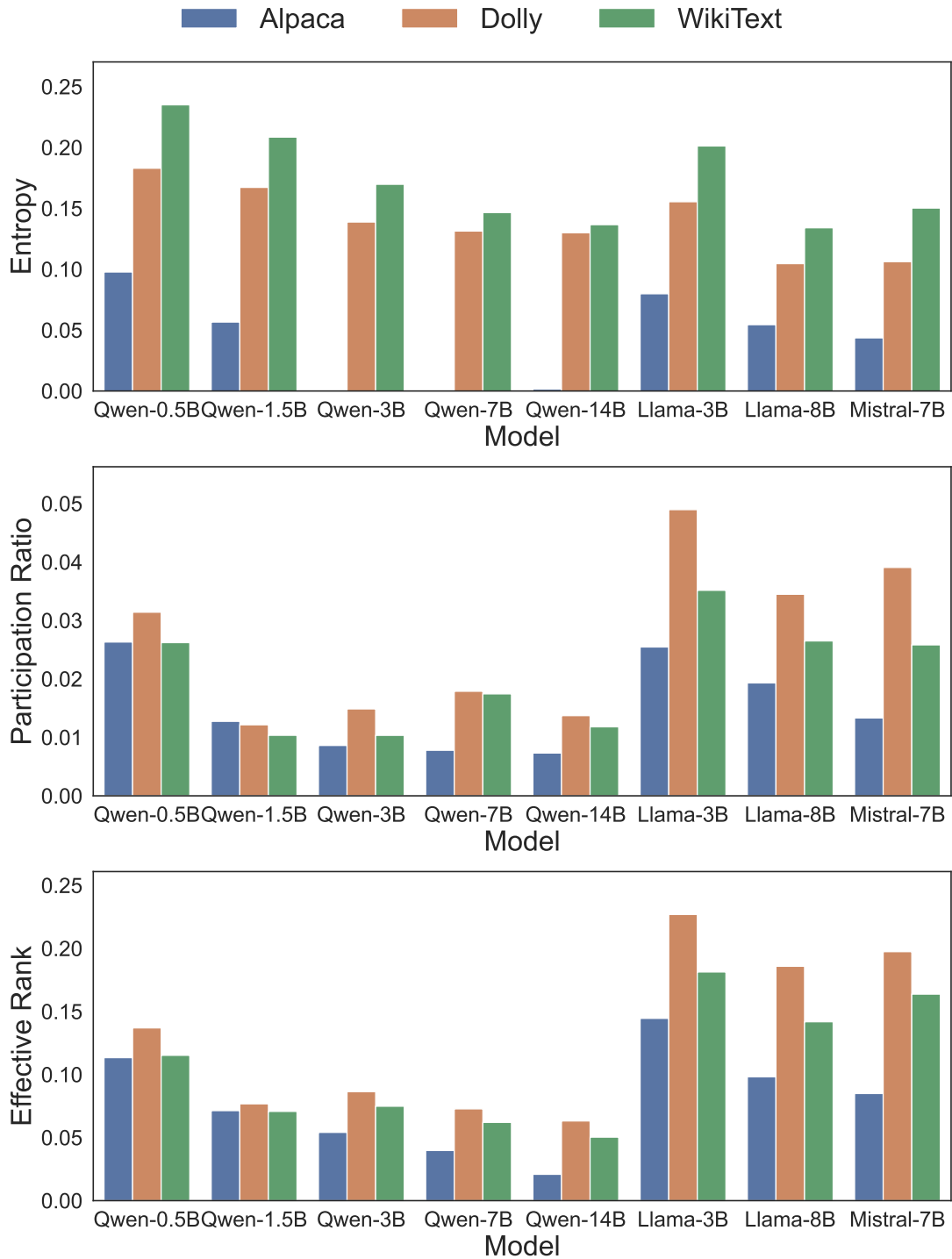


Figure 3. Comparison of LPP metrics – entropy, PR, and ER for different LLMs calibrated using three distinct calibration datasets: Alpaca, Dolly, and WikiText. Each subplot shows how a given metric varies across models for each dataset, using 100 samples per dataset. The top panel illustrates entropy trends, where models like Qwen-14B and Llama-3B show low entropy across datasets, indicating stable and confident predictions. In contrast, smaller models like Qwen-0.5B exhibit higher entropy and greater variability across datasets. The middle panel depicts the participation ratio, revealing that although absolute PR values vary slightly across datasets, models such as Llama-3B and Mistral-7B consistently maintain higher PR across datasets, suggesting a broader representational spread. The bottom panel on effective rank shows similar robustness: models with higher ER (e.g., Llama-3B) tend to preserve rank across datasets, indicating consistent use of internal dimensionality. Overall, while dataset choice can modestly affect absolute metric values, the relative ordering among models remains largely consistent, reinforcing that LPP metrics capture model-intrinsic representational dynamics rather than dataset-specific artifacts.

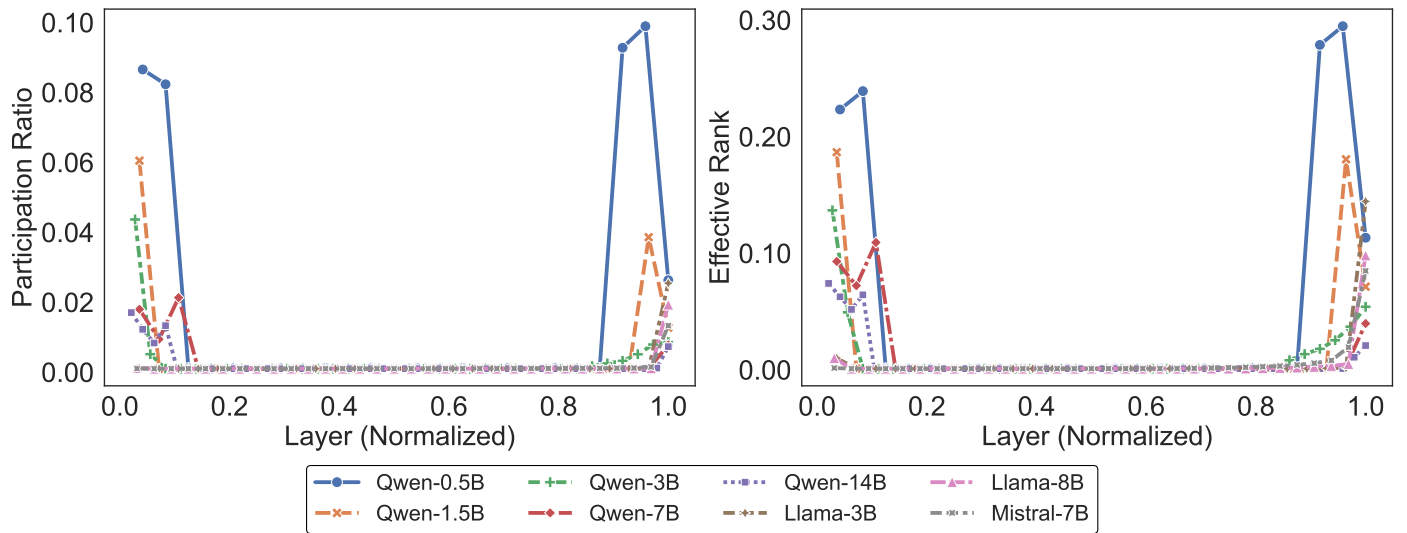


Figure 4. Layerwise sensitivity of LPP metrics – Participation Ratio (left) and Effective Rank (right) across normalized depth for a range of language models. Each curve corresponds to a different model, with layer depth normalized from input (0.0) to output (1.0). Across all models, both PR and ER display a distinctive “hourglass” profile: high values at the initial layers, dropping to a pronounced minimum in the middle, followed by a resurgence in the final layers. This consistent geometric trend reflects a compression-expansion representational structure within LLMs. Despite differences in scale and architecture, all models exhibit this emergent pattern, indicating that internal representational bottlenecks are a general feature of transformer-based LLMs. Notably, larger models (e.g., Llama-8B) tend to have lower middle-layer PR and ER compared to smaller ones, indicating more compact intermediate representations. These curves underscore the architectural universality of LPP dynamics and the utility of PR and ER as intrinsic probes of layerwise information geometry.

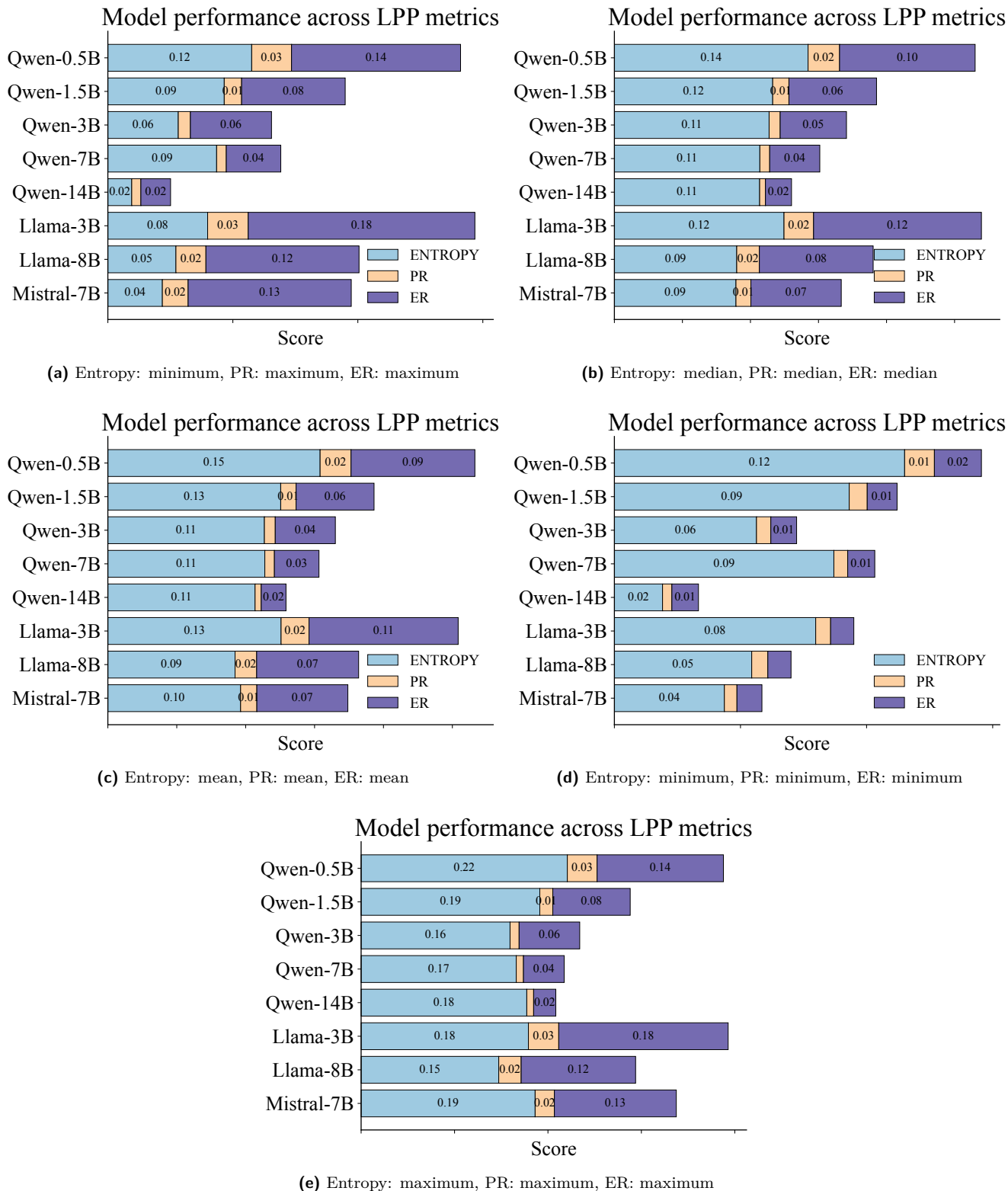
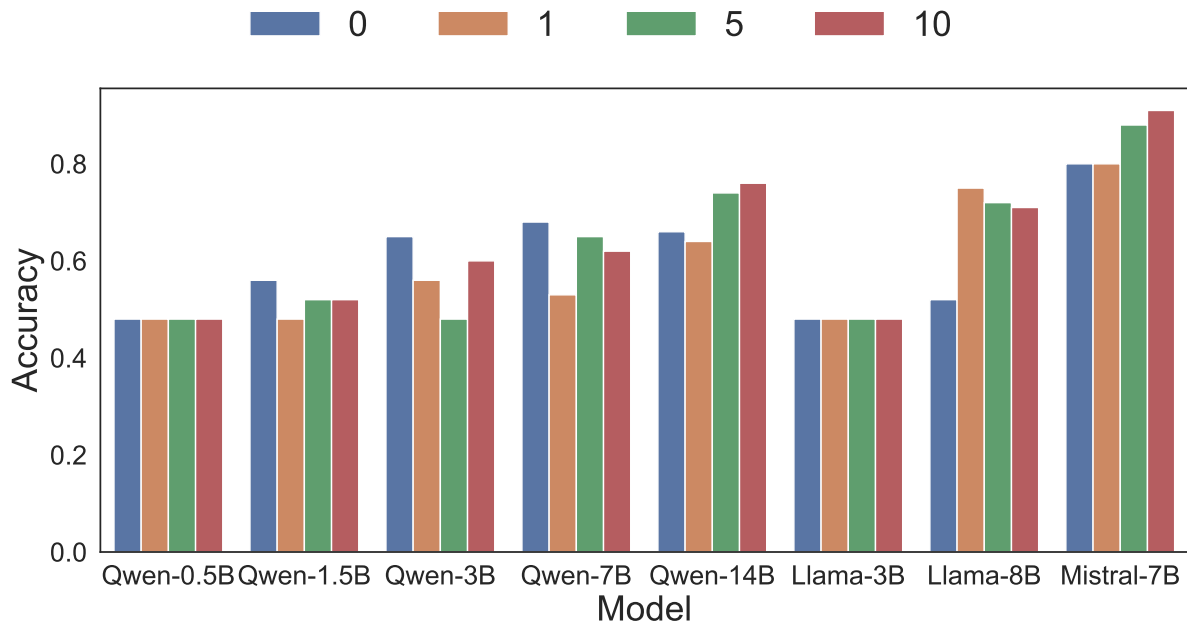
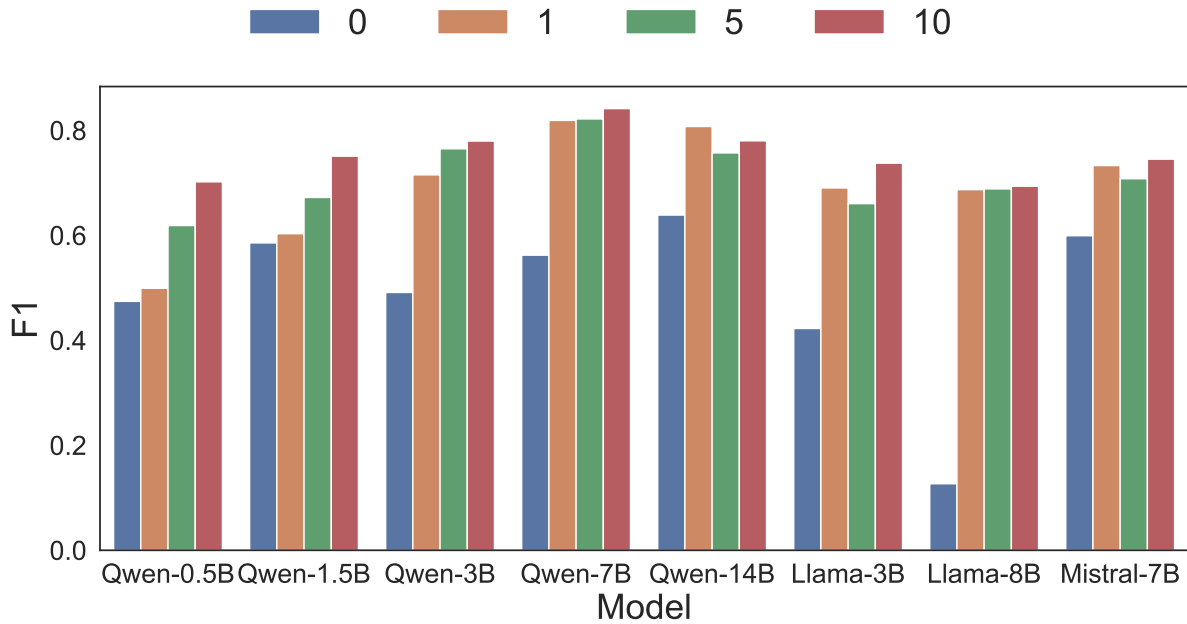


Figure 5. LPP metrics for different LLMs using five aggregation schemes: (a) entropy minimum, PR maximum, ER maximum; (b) all metrics aggregated via median; (c) all metrics aggregated via mean; (d) all metrics aggregated via minimum; (e) all metrics aggregated via maximum. Bars represent the aggregated score contribution from each metric (entropy, participation ratio, effective rank), revealing how summary statistics influence comparative model profiling. While the overall ranking remains broadly consistent across methods, specific models shift in relative prominence depending on the chosen aggregation method. This underscores the importance of transparent metric aggregation when interpreting latent diagnostic signals.



(a) Results on AR



(b) Results on SPC

Figure 6. Comparative analysis of how the number of in-context examples (0, 1, 5, and 10) influences the performance of various LLMs on synthetic tasks: AR and SPC. (a) illustrates model accuracy on AR tasks, showing a general trend of improved performance with an increasing number of in-context examples. (b) displays the F1 scores for SPC tasks, indicating more substantial performance gains for larger models like Qwen-14B and Mistral-7B when exposed to more examples. Smaller models (e.g., Qwen-0.5B) show more limited benefits from in-context learning. The consistent upward trend suggests that in-context examples significantly enhance a model’s ability to generalize and reason across both AR and SPC benchmarks, with larger models leveraging the added context more effectively.